Pheromone circuits and transcriptional cascades modulating transcriptional and chromatin states in the *Drosophila* central brain with social experience

Chengcheng Du [1], Jesús Emiliano Sotelo Fonseca [1], Lanling Jia [1], Shayna Scott [1], Sumie Okuwa [1], Sare Koruk [1], Corbin D. Jones [3], and Pelin C. Volkan [1, 2†]

[1]Department of Biology, Duke University, Durham, NC 27708, USA

[2]Department of Neurobiology, Duke University Medical Center, Durham, NC 27710, USA

[3]Department of Biology, University of North Carolina at Chapel Hill, Chapel Hill, NC 27599, USA

[†]Corresponding author: pelin.volkan@duke.edu

4341 French Family Science Center

124 Science Drive

Campus Box 90338, Duke University

Durham, NC 27708, USA

Abstract

Social experience significantly influences the behavioral and physiological responses of animals, including humans. In many animals, social isolation increases aggression, courtship, locomotion, and feeding while disrupting sleep. This occurs when peripheral neurons detect social signals, such as pheromones, which activate decision-making circuits in the brain. However, the molecular and circuit mechanisms of how chronic social isolation or enrichment alter gene expression and affect neuronal function and behavior remain unclear. In this study, we examined how transcription patterns and chromatin marks in male *Drosophila* brains change in response to social experience, and the effect of pheromone circuits and transcription factors involved in social circuit function. We focused on pheromone receptors Or47b and Or67d, as well as transcription factors Fru^M and Dsx^M. Our findings suggest that social experience affects multiple genes in the central brain. Disrupting Or47b, Or67d, Fru^M, and Dsx^M function moderated the transcriptional responses through antagonistic interactions. Specifically, Or47b circuits predominantly mediated transcriptional responses to social isolation through Dsx^M function, while Or67d and Fru^M regulated responses to group housing. Notably, mutants of fru^M and dsx^M exhibited more extensive transcriptional changes in the brain than Or mutants, especially for Fru^M/Dsx^M target genes. While social experience did not lead to detectable alterations in the overall chromatin profile in the whole brain, mutants of the four genes resulted in significant changes in the enrichment of H3K4me3 and RNA polymerase II (RNAPolII) compared to wild type. Furthermore, mutants in fru^M and dsx^M generally eliminated social experience-dependent changes in sleep and locomotion behaviors, whereas Or mutants exhibited more modest disruptions. Overall, our results uncover the pheromone circuits and transcriptional cascades in regulating molecular and behavioral responses to social experience.

Introduction

Across species, from invertebrates to mammals, social experience profoundly shapes behavior and physiology (Anders, 1978; Hoffman et al., 1975; Li et al., 2021; Luciano and Lore, 1975; Makinodan et al., 2012; Matsumoto et al., 2005; McGowan et al., 2009; Sánchez et al., 1998; Stagkourakis et al., 2020; Ueda and Kidokoro, 2002; Wang et al., 2022). Isolation disrupts cognitive processes such as sleep, memory, learning, and attention, while promoting maladaptive behaviors including aggression and excessive feeding (Brown et al., 2017; Cacioppo and Hawkley, 2009; Cacioppo et al., 2006; Cohen, 2004; Liu et al., 2025; Zelikowsky et al., 2018). In humans, these disruptions are associated with increased vulnerability to neuropsychiatric and neurodegenerative disorders (Cacioppo et al., 2015; Cacioppo et al., 2006; Cohen, 2004). Heightened awareness of these outcomes has led to the classification of social isolation and loneliness as a public health epidemic (General, 2023; Jeste et al., 2020; Lin, 2023). Yet, the molecular and circuit-level mechanisms mediating these effects remain largely unresolved.

Social experience has been shown to influence gene regulation in the nervous systems, from insects to mammals (Guerrero et al., 2020; Li et al., 2021; Robinson et al., 2008; Tung et al., 2012; Zhao et al., 2020). *Drosophila melanogaster*, as an excellent behavioral model, has been used to study many social behaviors, as well as behaviors influenced by social experience (Deanhardt et al., 2023; Ganguly-Fitzgerald et al., 2006; Goncharova et al., 2016; Li et al., 2021; Liu et al., 2011; Pan and Baker, 2014; Sethi et al., 2019; Ueda and Kidokoro, 2002; Ueda and Wu, 2009; Zhao et al., 2024; Zhao et al., 2020). *Drosophila* detects social cues by the peripheral neurons tuned to social cues like pheromones, which activate the pheromone and social circuits in the central brain, where information is integrated, and behavioral decisions are made (Fig. 1A). In the case of chronic social enrichment or isolation, the activity state of neuronal circuits activated by social experience, or lack thereof, likely alters gene expression at the transcription levels and chromatin patterns, ultimately adaptively modifying circuit function in the brain and behavioral outputs (Agrawal et al., 2019; Agrawal et al., 2020; Cushing and Kramer, 2005; Deanhardt et al., 2023; Flavell and Greenberg, 2008; Glastad et al., 2020; McGowan et al., 2009; Pan and Baker, 2014; Siuda et al., 2014; West and Greenberg, 2011; Wu et al., 2019; Zhao et al., 2020). Previous research on the *Drosophila* peripheral olfactory system demonstrated that social experience and pheromone receptor signaling modify chromatin states and alter the expression of numerous neuromodulatory genes, in addition to changing neuronal responses (Deanhardt et al., 2023; Sethi et al., 2019; Zhao et al., 2020). These findings suggest a strong link between social signals, transcriptional and chromatin modulation, and neuronal responses within the peripheral nervous system. Although there is clear evidence that social experience can alter gene regulation in the peripheral nervous system, the changes in gene expression and chromatin states in the central brain in different social contexts and the circuits that mediate these changes remain unclear (Fig. 1A).

In *Drosophila*, two transcription factors (TFs), Fruitless (Fru) and Doublesex (Dsx), regulate the development and function of sex-specific social circuits and social behaviors (Anand et al., 2001; Burtis and Baker, 1989; Dauwalder, 2011; Demir and Dickson, 2005; Hildreth, 1965; Kimura et al., 2008; Nagoshi et al., 1988; Neville et al., 2014; Rideout et al., 2010; Ryner et al., 1996; Stockinger et al., 2005; Villella and Hall, 1996). The male isoform of Fru, Fru^M, encodes a BTB zinc finger transcription factor involved in the sexual differentiation of neural circuits that control male behaviors (Ito et al., 1996; Ryner et al., 1996; Stockinger et al., 2005). In addition, fru^M is necessary for mediating social experience-dependent changes in male competitive copulation behaviors (Sethi et al., 2019). We also recently reported that changes in fru^M expression and function mediate social experience-dependent changes in courtship behaviors (Du et al., 2025). Fru was also shown to form a complex with the transcriptional cofactor Bonus (Bon), which recruits the chromatin regulators Histone deacetylase 1 (HDAC1) or

Heterochromatin protein 1a (HP1a) to regulate gene expression underlying neuronal sexual differentiation (Ito et al., 2012). In contrast, Dsx belongs to the evolutionarily conserved DMRT (Doublesex and Mab-3 Related Transcription factor) gene family. Sex-specific isoforms of Dsx (Dsx^M and Dsx^F) regulate sexual differentiation of both soma and the nervous system from invertebrates to vertebrates (Kopp, 2012; Murphy et al., 2007; Robinett et al., 2010). Perturbation of Dsx function changes courtship behavior in both males and females. Moreover, Dsx^M is necessary and sufficient for males to acquire experience-dependent courtship behavior in the absence of Fru^M. Both Fru^M and Dsx^M bind DNA to regulate the expression of overlapping sets of genes, although some genes are specifically regulated by either Fru^M or Dsx (Clough et al., 2014; Neville et al., 2014).

Fru^M is expressed in interconnected neurons that label circuits for mediating social behaviors such as courtship and aggression (Cachero et al., 2010; Jai et al., 2010; Vrontou et al., 2006). Fru^M positive neural circuits include peripheral neurons that detect social cues to neural centers for sensory processing, integration, and decision-making, as well as the descending motor pathways responsible for executing the behaviors (Dauwalder, 2011; Jai et al., 2010; Kimura et al., 2008; Lee et al., 2000; Neville et al., 2014; Stockinger et al., 2005; von Philipsborn et al., 2014). In the olfactory system, two classes of pheromone-sensing olfactory receptor neurons (ORNs) that express pheromone receptors Or47b and Or67d are fru^M positive (Jai et al., 2010; Stockinger et al., 2005). Or47b ORNs detect male and female pheromones and drive age and social experience-dependent male copulation advantage in a fru^M-dependent manner (Dweck et al., 2015; Lin et al., 2016; Sethi et al., 2019). Or67d ORNs detect male-specific pheromone 11-*cis*-vaccenyl acetate (*cis*-VA) and function to inhibit courtship behaviors in males (Ha and Smith, 2006; Kurtovic et al., 2007).

Previous studies demonstrated that social isolation alters many behavioral and physiological responses of *Drosophila,* increasing aggression, courtship, locomotion, and feeding, and disrupting sleep (Deanhardt et al., 2023; Ganguly-Fitzgerald et al., 2006; Goncharova et al., 2016; Li et al., 2021; Liu et al., 2011; Pan and Baker, 2014; Sethi et al., 2019; Ueda and Kidokoro, 2002; Ueda and Wu, 2009; Zhao et al., 2024; Zhao et al., 2020). In a related study, we demonstrated that changes in courtship behaviors, resulting from social experiences, are associated with alterations in the expression and function of fru^M, as well as specific circadian genes that are potential targets of Fru^M and/or Dsx^M (Du et al., 2025). Activating pheromone-sensing neurons through chronic exposure to social cues stimulates social circuits and engages the transcriptional functions of Fru^M and Dsx^M within these neurons.

Behavioral modulation in response to social experiences likely depends on detectors of social signals, such as pheromone receptors (like Or47b and Or67d), and regulators of social circuits like Fru^M and Dsx^M. To test this hypothesis, we conducted a study exploring how transcriptional and chromatin patterns in the brain change when we functionally disrupt these four pathways using male mutants in *Or47b*, *Or67d*, fru^M, and dsx^M raised in monosexual groups or in isolation (Fig. 1B). We additionally examined the impact of these mutants on social modulation of behaviors. Our results suggest that: 1) Social experience leads to changes in numerous genes involved in various processes, from metabolism to behavioral regulation, neural development, and immunity. Loss of *Or47b*, *Or67d*, fru^M, or dsx^M normalized the transcriptional responses to social experience, with general antagonistic effects between Or47b and Or67d pheromone circuits, and between Fru^M and Dsx^M circuits. We found trends where Or47b pheromone circuits and Dsx^M circuits function together in mediating transcriptional responses to social isolation, while Or67d neuronal circuits and Fru^M circuits function together to drive transcriptional responses to group housing in the brain. 2) Under the same housing conditions, compared to Canton-S wild type (*CS*), fru^M and dsx^M mutant brains showed more extensive changes at the transcriptional level than those observed in *Or47b* or *Or67d* mutants. Fru^M and Dsx^M function as either transcriptional repressors or activators, influencing downstream target genes. 3) Despite transcriptional changes, at the chromatin level, social experience does not significantly alter the overall distribution of H3K4me3 or

RNA polymerase II (RNAPolII) in the whole brain. However, compared to *CS*, the four mutants cause numerous changes to the enrichment of H3K4me3 or RNAPolII under the same social conditions. The transcriptional changes identified in different mutants are accompanied by modest concordant changes in H3K4me3 or RNAPolII enrichment. 4) Mutants in fru^{M} and dsx^{M} generally eliminate social experience-dependent changes in sleep and locomotion behaviors. In contrast, Or mutants exhibited more modest disruptions in social modulation of locomotion and courtship, with housing-specific defects observed in *Or47b* mutants. Our results identified pheromone circuits and transcriptional cascades that work with them in the modulation of molecular responses to social experience, which reprogram brain function and behaviors. These findings provide new insights into how social experiences affect molecular plasticity, laying the groundwork for future research on the molecular mechanisms linking social interactions to behavior and physiology.

Results

The contribution of pheromone receptors and social circuit regulators on transcriptional and chromatin responses to social experience in the brain

We recently reported differentially expressed genes (DEGs) between grouped and isolated *CS* male brains (Du et al., 2025). To explore the contribution of pheromone circuits and social circuit regulators in social modulation of gene expression, we analyzed transcriptional and chromatin profiles in *Or47b, Or67d,* fru^{M}, and dsx^{M} mutant brains from grouped or isolated males (Fig. 1A-B). We performed bulk RNA sequencing of brain tissues from group-housed (GH) and single-housed (SH) male *CS* wild type, and $Or47b^{2/3}$, $Or67d^{GAL4/GAL4}$, $fru^{LexA/4\text{-}40}$, and $dsx^{0683/1649}$ mutants (Fig. 1B). To explore potential chromatin-based mechanisms for social experience-dependent gene regulation, we additionally conducted CUT&RUN (Cleavage Under Targets and Release Using Nuclease) and sequencing in male brains using the same genotypes and social conditions to assess the genome-wide enrichment of two active chromatin marks: H3K4me3 and RNAPolII (Fig. 1B).

We first examined the quality of the sequencing results. From the PCA results of both RNA seq and CUT&RUN, samples with the same genotypes are clustered together (Fig. 1C, D, and E). Both the transcription profiling and chromatin landscape of $fru^{LexA/4\text{-}40}$ and $dsx^{0683/1649}$ mutants appeared more distinct from the wild-type *CS*, while $Or47b^{2/3}$ and $Or67d^{GAL4/GAL4}$ mutants showed more modest changes compared to the wild type (Fig. 1C, D, and E). Regarding the distribution of H3K4me3 and RNAPolII peaks, over 50% of the peaks for both marks were found around the promoter regions throughout the genome (Fig. 1F and G).

Normalized counts of RNA transcripts of several housekeeping genes or control genes (*RpS29*, *Hmt4-20*, and *TSG101*) appeared consistent across all genotypes (Supplementary Fig. 1A-C). $fru^{LexA/4\text{-}40}$ mutants significantly decreased the expression of *fru* (Supplementary Fig. 1E). Within the overall brain, *fru* expression showed very little to no change with social experience in *CS* or mutants. Yet, similar to results from the peripheral olfactory system (Deanhardt et al., 2023), we found some *fru* exons to be differentially regulated in *CS* with social experience (Fig. 1H frames). The same exons were also decreased in $Or67d^{GAL4/GAL4}$ mutants and $dsx^{0683/1649}$ mutants (Fig. 1H frames). $fru^{LexA/4\text{-}40}$ males exhibited a reduction in H3K4me3 and RNAPolII enrichment at the *fru* locus (Fig. 1H). $dsx^{0683/1649}$ mutants also exhibited decreased *dsx* expression, as well as H3K4me3 and RNAPolII enrichment at the *dsx* locus (Fig. 1I; Supplementary Fig. 1F).

184 These results show that Fru^M and Dsx^M have a more dramatic impact on the transcriptional and chromatin
185 responses to social experience, compared to the effect of Or47b and Or67d pheromone circuits.

186 Or47b and Or67d pheromone circuits function antagonistically to influence transcriptional 187 responses to social experience in the central brain

188 Compared to the SH *CS*, we found approximately 130 genes that are transcriptionally up- or
189 downregulated in GH *CS* (Fig. 2A; Fig. 4A, B). These DEGs are involved in many biological processes,
190 especially immunity, metabolism, receptor signaling, and behaviors (Fig. 2B; Fig. 3B; Supplementary
191 Fig. 4A; Supplementary Table 1). We first examined how pheromone circuits drive transcription
192 responses to social experience. Both $Or47b^{2/3}$ and $Or67d^{GAL4/GAL4}$ mutants showed a significant reduction
193 in the number of DEGs between GH and SH (Fig. 4A-C). $Or47b^{2/3}$ mutants predominantly disrupted DEG
194 patterns in response to social isolation (Fig. 2A). In contrast, in $Or67d^{GAL4/GAL4}$ mutants, DEG patterns in
195 response to group housing were disrupted (Fig. 2A). We also compared the Gene Ontology (GO) terms of
196 DEGs in GH/SH comparisons of *CS*, $Or47b^{2/3}$ and $Or67d^{GAL4/GAL4}$ mutants to determine if the two
197 pheromone circuits modulate different biological processes and molecular functions in response to social
198 experience (Fig. 2B). For example, DEGs related to immune functions in *CS* male brains were no longer
199 DEGs in $Or67d^{GAL4/GAL4}$ mutant brains (Fig. 2A, B). This suggests that Or67d circuits may contribute to
200 the transcriptional differences in immune genes between grouped and isolated wild-type male brains. In
201 $Or47b^{2/3}$ mutants, on the other hand, most specific changes are observed in GO terms for locomotion and
202 hormone activity (Fig. 2A, B).

203 We next investigated how chromatin states changed in response to different social experiences. The
204 overall distribution of either H3K4me3 or RNAPolII did not show any significant change between the
205 GH/SH housing comparison in any genetic background (Fig. 6D), including *CS*, which had the most
206 DEGs. Interestingly, multiple papers over the past two decades indicate that this is a relatively common
207 observation (Agrawal et al., 2019; Brovkina et al., 2021; Kiani et al., 2022). This discrepancy, where
208 DEGs are present without accompanying changes in chromatin marks, may be due to technical limitations
209 in detecting chromatin level changes that occur only in specific cell populations within the brain. These
210 localized changes might be masked when analyzing chromatin at the global level across the entire brain.
211 Furthermore, the hundreds to thousands of RNA transcripts produced from a single gene in the genome—
212 typically with only two copies in most cells—could also explain the absence of a significant change in
213 chromatin enrichment for H3K4me3 or RNAPolII around DEGs under varying social conditions.

214 The results indicate that Or67d circuits primarily influence transcriptional changes in response to group
215 housing. In contrast, Or47b circuits mainly drive transcriptional responses to social isolation, although
216 their impact on the social modulation of transcriptional profiles in the brain is relatively weaker (Fig. 2L).
217 These data highlight the differences and opposing functions of the two pheromone circuits in
218 implementing the effects of social experience on gene expression throughout the brain.

219 The effect of Or47b and Or67d pheromone circuits on gene expression and chromatin state 220 in the brain

221 In addition to investigating the contribution of pheromone circuits in mediating social modulation of
222 transcription, we next examined how pheromone circuits affected overall transcription under the same
223 social condition. When compared to *CS* under both GH and SH conditions, the $Or47b^{2/3}$ mutant changed
224 the expression of many supramolecular and cytoskeletal-related genes (Fig. 2C-F; Supplementary Fig. 5).
225 $Or67d^{GAL4/GAL4}$ mutant, on the other hand, altered the expression of various metabolic processes and
226 defense responses under GH conditions (Fig. 2C-D; Supplementary Fig. 5). Under SH conditions, the

227 *Or67d*$^{GAL4/GAL4}$ mutant mainly altered the expression of genes in molecular binding and metabolic
228 processes (Fig. 2E-F; Supplementary Fig. 5). Overall, the effect of disrupting Or67d and Or47b function
229 on transcriptional profiles in both GH and SH brains was specific to each pheromone circuit, with little
230 overlap between the mutants (Fig. 2C-F, Fig. 4G and K). These results agree with specific and
231 overlapping roles for each pheromone circuit in mediating distinct cellular and transcriptional responses
232 in the central brain.

233 We next investigated how chromatin states change when different pheromone circuits are disrupted. We
234 did not find significant differentially enriched peaks (DEPs) for H3K4me3 or RNAPolII in male brains
235 when comparing GH/SH housing conditions in any of the genotypes (Fig. 6D). However, loss of *Or47b*
236 or *Or67d* exhibited DEPs for H3K4me3 and RNAPolII when compared to *CS* under either GH or SH
237 conditions (Fig. 2G-K). The effect of Or47b or Or67d circuits on H3K4me3 and RNAPolII enrichment
238 compared to wild type in both GH and SH brains was generally specific (Fig. 2G-J). A small portion of
239 DEPs were altered in the same direction in both mutants, yet to different extents (Fig. 2G-J). To
240 determine the genes with DEPs, we linked the DEPs to the nearest genes (Fig. 2G-K). Next, we
241 performed GO term analysis on the genes with DEPs in *Or47b*$^{2/3}$ and *Or67d*$^{GAL4/GAL4}$ mutants compared to
242 wild type in either social condition (Fig. 2K). We found that *Or47b*$^{2/3}$ mutants altered the RNAPolII
243 distribution around genes involved in channel activity-related processes under the SH condition but not in
244 the GH condition (Fig. 2K). Genes with RNAPolII or H3K4me3 DEPs in *Or67d*$^{GAL4/GAL4}$ mutants were
245 not enriched for any GO terms.

246 We next extended the analysis to determine if the changes in DEPs were concordant with the changes in
247 DEGs. We compared DEGs to genes with DEPs that changed in the same direction in Or mutants
248 (Supplementary Fig. 2). The number of genes with DEPs was much less than that of DEGs. We identified
249 a few genes exhibiting concordant changes in transcription and enrichment patterns for either active mark.
250 The genes with concordant changes in *Or47b*$^{2/3}$ mutants are involved in various metabolic, catabolic, and
251 intracellular transport processes, and while in *Or67d*$^{GAL4/GAL4}$ mutants, they are involved in enzyme
252 activity, DNA, and chromosome regulation (Supplementary Fig. 2E-F). These results suggest that Or47b
253 and Or67d ORN circuits reprogram chromatin states and transcription around unique sets of genes in the
254 brain, highlighting potential differences in cellular responses driven by different pheromone circuits.

255 Fru^M and Dsx^M function antagonistically to influence transcriptional responses to social
256 experience in the central brain

257 The effect of Fru^M or Dsx^M on gene regulation in the nervous system, or their modes of transcriptional
258 regulation, remains unclear. We performed a similar analysis on *fru*$^{LexA/4-40}$ and *dsx*$^{0683/1649}$ mutant brains.
259 First, we investigated whether the function of Fru^M or Dsx^M is required to drive transcriptional changes to
260 social experience observed in the wild type using *fru*$^{LexA/4-40}$ and *dsx*$^{0683/1649}$ mutant males that are either
261 grouped or isolated. The expression pattern of DEGs in GH/SH comparisons in *CS* brains showed that
262 Fru^M and Dsx^M have opposing roles in mediating gene expression with social experience. In *fru*$^{LexA/4-40}$ or
263 *dsx*$^{0683/1649}$ mutants, the transcriptional differences between GH and SH are largely eliminated, albeit in
264 different ways (Fig.3A; Fig.4A-D). Specifically, the transcriptional profile in both GH and SH *fru*$^{LexA/4-40}$
265 mutant brains appeared similar to that of SH *CS* brains (Fig.3A), suggesting that Fru^M contributes to
266 mediating the transcriptional responses to GH. This pattern was opposite in *dsx*$^{0683/1649}$ mutant brains,
267 where, for many genes, transcriptional responses to isolation appeared more significantly disrupted
268 compared to GH (Fig.3A). This result indicates that, in contrast to Fru^M, Dsx^M plays a significant role in
269 mediating the transcriptional responses to SH. Fru^M or Dsx^M were previously shown to bind to the
270 regulatory elements of many of the DEGs (Fig. 4D) (Clough et al., 2014; Neville et al., 2014), suggesting
271 that the transcriptional defects observed are likely a direct downstream effect of the loss of Fru^M and

272 Dsx^M function. The fact that some of these DEGs were upregulated and others were downregulated in
273 $fru^{LexA/4-40}$ and $dsx^{0683/1649}$ mutants also reveals that both transcription factors (TFs) can function as
274 transcriptional repressors or activators in a gene-specific manner (Fig. 4D, H, L; Supplementary Fig. 6).
275 Alternatively, Fru and Dsx proteins can potentially form different homomeric or heteromeric complexes,
276 which determine repressor or activator functions on target genes as well as themselves, and mutations in
277 either *fru* or *dsx* can alter the stoichiometry of these complexes, determining their effects on transcription.

278 The total number of DEGs between GH and SH male brains is significantly lower in $fru^{LexA/4-40}$ or
279 $dsx^{0683/1649}$ mutants compared to that of wild-type male brains (Fig. 4A-C). A number of GO terms related
280 to metabolism and behavior from DEGs responding to social experience in *CS* were absent in $fru^{LexA/4-40}$
281 mutants (Fig.3A-B; Supplementary Table 1). Yet, the DEGs identified between GH and SH in $fru^{LexA/4-40}$
282 mutants are enriched in GO terms such as various receptor activities and binding processes (Fig. 3B;
283 Supplementary Fig. 4). The DEGs between grouped and isolated $dsx^{0683/1649}$ mutants were not enriched in
284 any GO terms but rather in defense response and cell communication Reactome or KEGG terms (Fig.3B;
285 Supplementary Fig. 4). In addition to the normalization of transcription in response to social experience in
286 $fru^{LexA/4-40}$ or $dsx^{0683/1649}$ mutants, the distribution of two active chromatin marks, H3K4me3 and
287 RNAPolII, did not show any significant changes between housing conditions in either mutant (Fig. 6D).
288 Overall, these data reveal opposing modes of regulation for Fru^M and Dsx^M in mediating transcriptional
289 responses to grouping and isolation in the brain, respectively (Fig. 3L).

290 The effect of Fru^M and Dsx^M function on gene expression and chromatin state in the brain

291 Next, we analyzed changes in transcription in $fru^{LexA/4-40}$ and $dsx^{0683/1649}$ mutant male brains compared to
292 the wild type under the same housing conditions (Fig. 3C-F), which can include genes directly regulated
293 by Fru^M and Dsx^M. DEGs in GH conditions from $fru^{LexA/4-40}$ mutant/*CS* or $dsx^{0683/1649}$ mutant/*CS*
294 comparison are involved in many metabolic pathways, oxidoreductase activity, structural processes, and
295 RNA processing (Fig. 3C-D; Supplementary Fig. 5). DEGs in SH conditions in $fru^{LexA/4-40}$ mutants include
296 genes involved in supramolecular and defense processes (Fig. 3E-F; Supplementary Fig. 5). In
297 comparison, SH $dsx^{0683/1649}$ mutants changed the expression of genes regulating cell-cell junctions and
298 communication, development of the nervous system, and various signaling pathways (Fig. 3E-F;
299 Supplementary Fig. 5). Overall, transcriptional profiles in both GH and SH brains revealed some genes to
300 be exclusively impacted in either $fru^{LexA/4-40}$ or $dsx^{0683/1649}$ mutants, while others were affected in both
301 mutants. These results suggest that distinct and shared transcriptional responses in the central brain are
302 mediated by Fru^M and Dsx^M.

303 Under the same housing condition, H3K4me3 or RNAPolII displayed differential distribution in $fru^{LexA/4-}$
304 ^{40} or $dsx^{0683/1649}$ mutants compared to *CS* in male brains (Fig. 3G-K; Fig. 6). Genes linked with H3K4me3
305 or RNAPolII DEPs were enriched in diverse GO terms (Fig. 3K). The $dsx^{0683/1649}$ mutants exhibited
306 varying levels of H3K4me3 enrichment near genes related to DNA catalytic activity compared to *CS*
307 under the GH condition, and showed differential enrichment of RNAPolII around genes involved in
308 mating and reproductive behaviors, developmental and metabolic processes (Fig. 3K). While $fru^{LexA/4-40}$
309 mutants showed differential enrichment of RNAPolII at genes involved in synapse assembly or
310 organization in the GH condition (Fig. 3K). $fru^{LexA/4-40}$ and $dsx^{0683/1649}$ mutants show both specific and
311 shared influences on chromatin states in each housing condition compared to wild type (Fig. 3G-J).
312 Consistent with their unique and shared roles in transcriptional regulation, these data continue to support
313 distinct housing-specific changes in chromatin profiles around each gene mediated by Fru^M and Dsx^M.

314 The comparison of DEGs and genes with DEPs in $fru^{LexA/4-40}$ and $dsx^{0683/1649}$ mutants relative to *CS*
315 revealed concordant changes at both transcription and chromatin levels, specifically regarding H3K4me3

316 or RNAPolII enrichment. Notably, a significant number of genes with H3K4me3 DEPs in *dsx*$^{0683/1649}$
317 mutants corresponded to changes in transcription levels in the same direction, including many genes
318 related to behaviors and DNA processes (Supplementary Fig. 3). Interestingly, *fru*$^{LexA/4-40}$ and *dsx*$^{0683/1649}$
319 mutants changed both the transcript level and chromatin level for circadian and sleep-related genes, *per*
320 and *sand* (Supplementary Fig. 3; Fig. 7). Strikingly, the *sand* gene displayed dramatically decreased
321 H4K3me3 enrichment and transcript level in *fru*$^{LexA/4-40}$ and *dsx*$^{0683/1649}$ mutants, with the RNAPolII
322 binding level remaining the same (Supplementary Fig. 9). This might suggest either transcriptional
323 priming or RNAPolII pausing at the *sand* gene locus in *fru*$^{LexA/4-40}$ and *dsx*$^{0683/1649}$ mutants, possibly due to
324 the lack of H3K4me3 enrichment.

325 Or47b circuit functions through Dsx^{M} in response to social isolation, whereas Or67d circuit 326 functions through Fru^{M} in response to group housing

327 Our analyses have shown that *Or47b*$^{2/3}$, *Or67d*$^{GAL4/GAL4}$, *fru*$^{LexA/4-40}$, and *dsx*$^{0683/1649}$ mutants all normalized
328 the transcriptional differences between GH and SH comparison in unique ways (Fig. 2-4; Supplementary
329 Fig. 7). Activation of pheromone-sensing neurons in the olfactory system activates ensembles of neurons
330 within circuits driving social behaviors. This circuit activation can engage the functions of Fru^{M} and Dsx^{M}
331 transcription factors expressed in a pheromone circuit-specific way to mediate the transcriptional and
332 chromatin effects of social experience in the brain. To determine the neural and transcriptional cascades
333 involved in this process and identify shared genes that are co-regulated by each pheromone circuit
334 alongside Fru^{M} and Dsx^{M}, we compared the DEGs and DEPs in each mutant (Fig. 4-6).

335 All mutants decreased the number of social experience-dependent DEGs in unique ways (Fig. 4A-D). In
336 both *Or47b*$^{2/3}$ and *dsx*$^{0683/1649}$ mutants, the patterns of DEGs in response to social isolation are disrupted
337 (Fig. 4D). This suggests that the Or47b circuits and Dsx^{M} are important for driving transcriptional
338 responses to isolation. Notably, *dsx*$^{0683/1649}$ mutants show a more significant defect in social experience-
339 induced transcriptional changes, both in terms of the number of genes affected and the level of
340 transcriptional change observed (Fig. 4A-D). In contrast, in *Or67d*$^{GAL4/GAL4}$ and *fru*$^{LexA/4-40}$ mutants,
341 transcriptional responses to group housing were largely disrupted (Fig. 4D), suggesting that Or67d
342 circuits and Fru^{M} drive transcriptional responses to group housing. Again, *fru*$^{LexA/4-40}$ mutants exhibited a
343 stronger defect in transcription. Notably, *Dsk*, which encodes a neuropeptide involved in regulating
344 aggression and suppressing courtship behaviors (Agrawal et al., 2020; Wu et al., 2019), is the only gene
345 statistically unaltered between grouped and isolated male brains across all wild-type and mutant
346 genotypes (Fig. 4C; Supplementary Fig. 1D).

347 Comparing each mutant to *CS* under the GH condition revealed that *Or47b*$^{2/3}$ mutants showed the least
348 number of DEGs among other mutants (Fig. 4E-F). In contrast, under the SH condition, *Or67d*$^{GAL4/GAL4}$
349 mutants showed the least number of DEGs compared to *CS* (Fig. 4I-J). With respect to wild-type brains,
350 *fru*$^{LexA/4-40}$ mutants or *dsx*$^{0683/1649}$ mutants always had more dramatic effects on transcriptional profiles
351 compared to Or mutants (Fig. 4E-L), supporting the hypothesis that *fru*- or *dsx*-positive central circuits
352 likely integrate information from multiple pheromone circuits unexplored in this study.

353 We next aimed to determine whether we could identify functionally shared or segregated pathways
354 connecting different pheromone circuits to the Fru^{M} and Dsx^{M} transcriptional functions in the central
355 brain. We compared the DEGs in Or mutants to those in TF mutants versus *CS*. *Or47b*$^{2/3}$ mutants had a
356 large number of DEGs that uniquely overlapped (268) with *dsx*$^{0683/1649}$ mutants under the SH condition
357 (Fig. 4K). Meanwhile, a large number of DEGs in *Or67d*$^{GAL4/GAL4}$ and *fru*$^{LexA/4-40}$ mutant brains uniquely
358 overlapped (197) in the GH condition (Fig. 4G). Among all the DEGs from comparisons of any mutant
359 versus *CS*, a notable number showed altered expression in the same direction across all four mutants, or

exhibited unique directional changes in specific mutants (Fig. 5). A significant number of the remaining DEGs showed interesting overlaps in expression patterns between Or (*Or47b* or *Or67d*) and TF (fru^{M} or dsx^{M}) mutants. We generally observed a trend indicating that, in both GH and SH conditions, the transcriptional effects on DEGs seen in $Or47b^{2/3}$ mutants are largely similar to those in $dsx^{0683/1649}$ mutants, and occasionally to $fru^{LexA/4\text{-}40}$ mutants (Fig. 5 gray frames). We saw opposing trends with $Or67d^{GAL4/GAL4}$ mutants, where the transcriptional effects generally aligned with $fru^{LexA/4\text{-}40}$ mutants, and occasionally with $dsx^{0683/1649}$ mutants (Fig. 5 gray frames).

DEGs that changed in various combinations of directions were enriched in distinct GO terms (Fig. 5). Though DEGs showed enrichment for specific biological processes, molecular functions or cellular components in each mutant, under both housing conditions, DEGs in $Or47b^{2/3}$ and $dsx^{0683/1649}$ mutants shared many of the top ranked GO and KEGG terms (Supplementary Fig. 5). In contrast, DEGs in $Or67d^{GAL4/GAL4}$ and $fru^{LexA/4\text{-}40}$ mutants showed overlaps in GO and KEGG terms (Supplementary Fig. 5). These results highlighted potential functional connections between Or47b and Dsx^{M} neuronal circuits, particularly in isolated males, and between Or67d and Fru^{M} neuronal circuits especially in grouped males, suggesting that Or47b circuits might communicate with *dsx*- positive neurons in response to social isolation whereas Or67d circuits might function through *fru*-positive neural circuits in response to social enrichment.

At the chromatin level, genes with H3K4me3 or RNAPolII DEPs were mostly unique to each mutant, showing modest overlap with other genotypes (Fig. 6A-B). These genes were associated with distinct GO terms that were more genotype-specific (Fig. 6C). Figure 7 summarizes genes exhibiting concordant changes in both transcription and chromatin state (H3K4me3 or RNAPolII) in the same direction in each genotype. These findings suggest that transcriptional changes in these genes may be driven, at least in part, by broader chromatin remodeling events in the male brain induced by activation of different pheromone circuits in response to social experience, as well as the functions of Fru^{M} and Dsx^{M}.

Differential effects of pheromone circuits, Fru^{M}, and Dsx^{M} on the social modulation of Fru^{M}/Dsx^{M} target gene expression

Our results suggest that prolonged activation of pheromone circuits impacts the transcriptional activity of Fru^{M} or Dsx^{M}-expressing neurons associated with sex-specific and/or social behaviors. This likely leads to changes in the expression of Fru^{M} and/or Dsx^{M} downstream target genes, contributing to the social modulation of behaviors. A comparison of Fru^{M} and Dsx^{M} binding sites in the genome revealed overlap among the genes regulated by either Fru^{M} or Dsx^{M} (Fig. 4D, H, L; Supplementary Fig. 6A-B) (Clough et al., 2014; Neville et al., 2014). Our analysis identified genes that are exclusively regulated/co-regulated by Fru^{M} and Dsx^{M} (Supplementary Fig. 6), which have various functions, including neural development and function, as well as modulation of circadian rhythms, metabolic processes, and signaling pathways (Clough et al., 2014; Neville et al., 2014).

We first analyzed the effect of housing on Fru^{M} and Dsx^{M} target DEGs, and how they changed in $fru^{LexA/4\text{-}40}$ mutants and $dsx^{0683/1649}$ mutants. We found that many of the Fru^{M}/Dsx^{M} target genes were misexpressed primarily under one housing condition. Generally, $fru^{LexA/4\text{-}40}$ mutants exhibited defects in GH, while $dsx^{0683/1649}$ mutants showed defects in SH (Supplementary Fig. 6A). These DEGs contain binding sites for either Fru^{M} or Dsx^{M}, or both, in their regulatory elements (Supplementary Fig. 6A). Under the same housing conditions, some of the target DEGs were either up- or down-regulated in the same direction in both mutants, albeit generally with one mutant having a more dominant effect (Supplementary Fig. 6B-D). While many co-regulated DEGs showed changes in the same direction, others were affected in opposite directions (Supplementary Fig. 6B-D). Some of the target DEGs were regulated exclusively by

404 either Fru^M or Dsx^M (Supplementary Fig. 6B-D). These data suggest that social experience-induced
405 changes in Fru^M/Dsx^M target DEGs are mainly influenced by Fru^M in group-housed conditions, while
406 Dsx^M primarily drives responses to social isolation. Furthermore, they reveal both similarities and
407 differences in the mode of transcriptional regulation between Fru^M and Dsx^M on the expression of their
408 target genes, where both can function as activators or repressors of transcription.

409 To map the neural pathways from the olfactory pheromone-sensing neurons to the regulation of Fru^M,
410 Dsx^M and their target DEGs in the central brain, we compared the log2 fold change of these DEGs in
411 *Or47b*$^{2/3}$ and *Or67d*$^{GAL4/GAL4}$ mutants as well. The effects of *Or47b*$^{2/3}$ and *Or67d*$^{GAL4/GAL4}$ mutants on the
412 Fru^M/Dsx^M target DEGs were not as dramatic as *fru*$^{LexA/4-40}$ or *dsx*$^{0683/1649}$ mutants (Supplementary Fig. 6B-
413 D). We identified some DEGs that were either altered in the same direction in all 4 mutants, or in the
414 opposite direction only in a single mutant (Supplementary Fig. 6C-D). Similar to prior results, in both GH
415 and SH conditions, *Or47b*$^{2/3}$ mutants show transcriptional effects on target DEGs similar to *dsx*$^{0683/1649}$
416 mutants, and occasionally with *fru*$^{LexA/4-40}$ mutants (Supplementary Fig. 6C-D). In contrast, *Or67d*$^{GAL4/GAL4}$
417 mutants generally align with *fru*$^{LexA/4-40}$ mutants, and occasionally *dsx*$^{0683/1649}$ mutants (Supplementary Fig.
418 6C-D). These results are in agreement with the results above that suggest Or47b and Or67d circuits
419 predominantly work through Fru^M and Dsx^M, respectively.

420 In an accompanying study, we discovered that social experience influences the expression of circadian-
421 related genes (i.e., *cry, Clk, Pdf,* and *Sik3*) in the central brain (Du et al., 2025). Interestingly, many of
422 these circadian genes are Fru^M/Dsx^M target genes with Fru^M and/or Dsx^M binding in their upstream
423 regulatory elements (Clough et al., 2014; Neville et al., 2014). Due to the pleiotropic effects of the
424 circadian system on behavior and physiology, social experience-dependent alterations in Fru^M/Dsx^M
425 transcriptional cascades and the expression of downstream target circadian genes may drive the impact of
426 social experiences on behaviors. Indeed, knockdown of *fru*^{M} and mutants in various circadian genes either
427 amplified or reduced the effects of group housing-driven changes in courtship (Clough et al., 2014;
428 Neville et al., 2014). These results indicate that changes in circadian gene expression, influenced by social
429 experience, may arise as a consequence of alterations in the levels or functions of Fru^M or Dsx^M. To test
430 this hypothesis and more strictly temporally control transcriptional changes in circadian genes, we
431 sampled RNA at ZT7-8 from grouped and isolated male heads in different mutants and performed qRT-
432 PCR for *Clk, tim,* and *cry* with control genes (*TSG101*, *RpS29*, *Hmt4-20*, and *Dsk*). We found that
433 expression of *Clk* and *cry* trended towards an increase in response to isolation (Supplementary Fig. 8A)
434 (Du et al., 2025). Under both social conditions, *tim* and *cry* showed a decrease in *dsx*$^{0683/1649}$ mutants
435 (Supplementary Fig. 8B). *Or67d*$^{GAL4/GAL4}$ mutants showed the strongest decrease in the expression of *cry*,
436 in the same direction as observed in *dsx*$^{0683/1649}$ mutants (Supplementary Fig. 8B). *dsx*$^{0683/1649}$ mutants also
437 showed a slight increase in *Clk* expression in GH brains, which eliminated the difference in *Clk*
438 expression observed between GH and SH *CS* brains (Supplementary Fig. 8A-B). In contrast, in *fru*$^{LexA/4-40}$
439 mutants, *cry* expression decreased in SH brains, while *tim* expression increased in GH brains
440 (Supplementary Fig. 8B). These results suggest that Fru^M and Dsx^M differentially regulate their target
441 genes, i.e., circadian genes, in the head, and social experience can modulate the expression of the
442 circadian genes in response to the differential activation of different pheromone circuits and
443 transcriptional function of Fru^M and Dsx^M.

444 Differential effects of pheromone circuits, Fru^M, and Dsx^M on social modulation of
445 behaviors

446 Considering the transcriptional changes in the brains of mutants of *Or67d*, *Or47b*, *fru*^{M}, and *dsx*^{M}, we
447 wanted to explore their effects on the social modulation of behaviors. Disrupting the function of Or47b or
448 Or67d affects the detection of diverse social cues, while loss of Fru^M and Dsx^M function disrupts the

processing of social signals in the central social circuits (Dauwalder, 2011; Dweck et al., 2015; Ha and Smith, 2006; Kurtovic et al., 2007; Lin et al., 2016; Vrontou et al., 2006; Yamamoto and Koganezawa, 2013). Previous studies have shown that social experience can reset the circadian clock in *Drosophila*, and grouped *CS* males show increased sleep and decreased locomotion compared to isolated *CS* males (Levine et al., 2002; Li et al., 2021; Zhao et al., 2024). Therefore, we assessed sleep and locomotion activity in $Or47b^{2/3}$, $Or67d^{GAL4/GAL4}$, $fru^{LexA/4\text{-}40}$, and $dsx^{0683/1649}$ mutants to determine their contribution to social experience-dependent changes in behaviors (Fig. 8; Supplementary Fig. 10). We confirmed that GH *CS* males increased sleep and decreased locomotion compared to SH *CS* males (Fig. 8A-D). Both $fru^{LexA/4\text{-}40}$ and $dsx^{0683/1649}$ mutants diminished the differences in total sleep and locomotion between GH and SH males (Fig. 8A-D), indicating that they both play a role in the social modulation of these behaviors. In $dsx^{0683/1649}$ mutants, such elimination resulted from both a decreased GH sleep level and an increased SH level (Supplementary Fig. 10A-D). In $fru^{LexA/4\text{-}40}$ mutants, the sleep pattern showed a general decline in GH (Supplementary Fig. 10A-D). We also noted further differences in the transition of sleep from nighttime to daytime in $fru^{LexA/4\text{-}40}$ mutants (Fig. 8A). In particular, the activity bout at the transition from nighttime to daytime was not disrupted in $fru^{LexA/4\text{-}40}$ mutants as in other genotypes (Fig. 8A). This also agrees with their locomotion performance, in which $fru^{LexA/4\text{-}40}$ mutants showed an overall decrease in activity peaks in the transition, and a less significant difference in locomotion between SH and GH flies (Fig. 8C). $Or47b^{2/3}$ and $Or67d^{GAL4/GAL4}$ mutants did not dramatically alter sleep patterns or trends between GH and SH (Fig. 8A-B). However, $Or47b^{2/3}$ mutants decreased locomotion in SH flies (Fig. 8C-D; Supplementary Fig. 10E-H). This result aligns with transcriptional disruptions in genes involved in locomotion of $Or47b^{2/3}$ mutants in SH brains (Fig. 2B). These findings suggest that Fru^M and Dsx^M play essential but distinct roles in the social modulation of sleep and locomotion behaviors in isolated and grouped flies, with a potential role for Or47b in mediating changes in locomotion in SH flies.

Since Or47b, Or67d, Fru^M, and Dsx^M circuits are all related to courtship behaviors, we also performed single-pair male-female courtship assays to determine their effect on social modulation of courtship. Previous studies and our accompanying study showed that fru^M and dsx^M are necessary for normal courtship behaviors in male flies, and fru^M expression in the central brain neurons is necessary for mediating the social experience-induced changes in male courtship behaviors (Du et al., 2025). The role of fru^M regulation with social experience is diverse: in some neurons, altered Fru^M function enhances courtship behavior in SH males, while in other neurons it decreases courtship in response to GH (Du et al., 2025). Since social experience can influence gene regulation and behavior, and given that mutations in *Or47b* and *Or67d* affect the transcriptional profile and chromatin state of wild-type brains, we investigated whether either the Or47b or Or67d pheromone circuits play a role in how social experience modulates courtship behaviors. We quantified male courtship behaviors in *CS*, $Or47b^{2/3}$ and $Or67d^{GAL4/GAL4}$ mutants (Fig. 8E). Loss of *Or47b* function increased courtship in GH mutant males, though it did not completely eliminate the difference between GH and SH (Fig. 8E). The $Or67d^{GAL4/GAL4}$ mutants did not alter the courtship vigor in either social context (Fig. 8E). These results suggest that Or47b circuits contribute to courtship suppression in grouped males. Overall, our results suggest unique contributions of olfactory pheromone pathways and transcription factors critical for integrating social information on transcriptional and chromatin profiles are accompanied by equally unique effects on social modulation of various behaviors.

Discussion

492 A substantial body of evidence demonstrates that social environments, whether isolation or enrichment,
493 have lasting consequences for cognition, physiology, and behavior (Cacioppo and Hawkley, 2009; Dow-
494 Edwards et al., 2019; Jeste et al., 2020). Loneliness, in particular, has been consistently linked to
495 heightened risk and severity of neuropsychiatric and neurodegenerative disorders, establishing it as a
496 pressing public health concern (General, 2023; Jeste et al., 2020; Lin, 2023). Nevertheless, while the
497 behavioral outcomes of different social experiences are well recognized, the molecular pathways and
498 neural circuits mediating these effects remain insufficiently understood. In this study, we investigated
499 how transcription patterns and chromatin marks in the brains of male *Drosophila* change in response to
500 social experience. To determine the neural and transcriptional pathways responding to social experience,
501 we examined mutants in two pheromone receptors, Or47b and Or67d, along with two transcription
502 factors, Fru^M and Dsx^M, that influence sex-specific and social behaviors. The results show that $Or47b^{2/3}$,
503 $Or67d^{GAL4/GAL4}$, $fru^{LexA/4-40}$, and $dsx^{0683/1649}$ mutants significantly reduced the transcriptional responses to
504 social experience, suggesting that social modulation of gene expression involves all four genes and their
505 associated circuits. $Or47b^{2/3}$ and $Or67d^{GAL4/GAL4}$ mutants exhibited opposing effects on DEGs that are
506 altered by social experience in wild type. Similar opposing functional effects were also observed in
507 $fru^{LexA/4-40}$ and $dsx^{0683/1649}$ mutants. We found functionally segregated transcriptional cascades from
508 individual pheromone circuits that engaged the function of either Fru^M or Dsx^M in the central brain.
509 Mainly, we found that Or47b circuits generally function through Dsx^M in response to isolation, while
510 Or67d circuits work in group-housed males through Fru^M to mediate social experience-dependent
511 modulation of transcriptional responses. The RNA profiles from the brains of $fru^{LexA/4-40}$ and $dsx^{0683/1649}$
512 mutants also helped us identify both activation and repression functions for Fru^M and Dsx^M, in addition to
513 their shared and exclusive functions in mediating their effects on gene expression and behaviors in
514 different housing conditions. And finally, we found that social experience-dependent changes in sleep and
515 locomotion are generally eliminated in $fru^{LexA/4-40}$ and $dsx^{0683/1649}$ mutants, with moderate effects of
516 pheromone receptors on some of the behaviors under certain social conditions. Given that many of the
517 DEGs are direct targets of Fru^M and/or Dsx^M, our study reveals how changes in social and pheromone
518 circuit activity with social experience can alter transcriptional cascades reprogramming brains and
519 behaviors.

520 One surprising finding from our study is that, although we identified DEGs between grouped and isolated
521 male brains of wild-type flies, we did not observe dramatic changes in chromatin patterns of H3K4me3
522 and RNAPolII across any of the genotypes under different housing conditions. However, we detected
523 numerous changes to the enrichment of H3K4me3 and RNAPolII in each mutant compared with wild-
524 type brains under the same housing conditions. Some of these changes in chromatin were accompanied by
525 concordant changes at the transcription level. Combinatorial function of multiple histone modifications
526 together with RNAPolII is thought to be intimately connected to transcriptional states (Goldberg et al.,
527 2007; Jenuwein and Allis, 2001; Schones and Zhao, 2008). For instance, H3K4me3 and H3K27ac are
528 considered marks for actively transcribed genes, while H3K27me3 is enriched around transcriptionally
529 repressed genes (Boros, 2012; Lawrence et al., 2016; Schones and Zhao, 2008; Zhang et al., 2021; Zhou
530 et al., 2011). However, many studies have also shown discrepancies between the enrichment of specific
531 chromatin marks and transcription responses (Agrawal et al., 2019; Brovkina et al., 2021; Kiani et al.,
532 2022). For example, circadian analysis of transcriptional and chromatin states in mammalian cells
533 throughout the day revealed that such correlations might represent an oversimplified view (Koike et al.,
534 2012). This study found that while both transcription and chromatin states displayed circadian patterns,
535 numerous genes exhibited changes in chromatin patterns without affecting transcription levels and vice
536 versa. Comparison of transcriptional changes and histone marks in dopaminergic neurons in flies raised in
537 grouped versus isolated conditions also revealed only a small correlation in a limited number of genes

538 (Agrawal et al., 2019). They also discovered that many highly expressed genes showed unexpected
539 increases in the enrichment of the repressive H3K27me3 mark, alongside decreases in active chromatin
540 marks (Agrawal et al., 2019). Similarly, chromatin accessibility and gene expression in *fru*+ versus *fru*-
541 cells sorted from male and female fly brains show little overlap (Brovkina et al., 2021).

542 There are several explanations for the discrepancy we and others observe in transcript levels and
543 chromatin mark enrichment. One possibility is cellular heterogeneity. Changes in chromatin states may
544 occur in a small subset of cells in response to social experience. However, when analyzing the whole
545 brain, these subtle changes can be obscured by other cells where such changes are not happening. Single-
546 cell multiome ATAC and gene expression profiling techniques can simultaneously determine gene
547 expression and chromatin landscape from the same cell, potentially increasing the resolution and
548 confidence of molecular analysis (Yamagishi et al., 2024). An alternative explanation considers the
549 transcriptional and chromatin states of a gene as it transitions through active, repressed, and poised states.
550 Each of these states may be triggered by complex combinations of chromatin marks that accumulate
551 around genes as cells respond to various signals and pathways. Transitioning between active and
552 repressed transcriptional states may involve intermediate states as chromatin modifications build up
553 around responsive genes. These conditions could lead to intermediate states where transcription decreases
554 alongside an increase in repressive marks, while active marks remain unchanged. Conversely,
555 transcription might increase due to the loss of a repressive mark, rather than the gain of an active mark. In
556 this study, we only investigated two active marks, yet marks for repressed/closed chromatin are also
557 crucial for regulating gene expression. Studies on mammalian cells demonstrated that the promoters of
558 some transcriptionally repressed genes were marked with both active (H3K4me3) and repressive
559 (H3K27me3) epigenetic marks (Mikkelsen et al., 2007). These and numerous other studies indicate that
560 chromatin states, as signaled by histone marks or accessibility, only offer a probabilistic prediction of
561 transcription (Corbett, 2018; Fu et al., 2025). Changes in gene expression result from the combined
562 regulation of various factors, including chromatin accessibility, histone modifications, transcription
563 factors, and post-transcriptional modifications (Corbett, 2018; Fu et al., 2025). Comprehensive studies
564 that analyze gene expression across all features will lead to a better understanding.

565 Despite the discrepancy in chromatin and transcriptional states, we did identify a small list of genes with
566 concordant changes in transcript levels and active chromatin mark enrichment, like the *sand* gene. The
567 *sand* gene, which encodes a KCNK18/TRESK homolog potassium channel, plays a crucial role in
568 regulating various aspects of *Drosophila* behavior and physiology. It is involved in sleep regulation
569 within the dorsal fan-shaped bodies (Pimentel et al., 2016) and cardiac function (Abraham et al., 2018).
570 Additionally, it has been shown to operate in cortical glial cells to help control stress-induced seizures
571 (Weiss et al., 2019). Considering the important role of the *sand* gene and the notable alterations in its
572 transcriptional and chromatin state in $fru^{LexA/4\text{-}40}$ and $dsx^{0683/1649}$ mutants, it is possible that Sand may play a
573 role in mediating some of the impaired neural, behavioral, and physiological processes observed in these
574 mutants. Further studies are necessary to explore this hypothesis.

575 In a related paper, we demonstrated that the expression of fru^{M} and core circadian genes, which are
576 potentially regulated by Fru^{M} and Dsx^{M}, is altered by social experience and essential for changes in
577 courtship behaviors (Du et al., 2025). These results suggest that social experience might exert its effect on
578 behavioral modulation through changes in circadian state. In this study, we further strengthen these
579 findings by highlighting the roles of both Fru^{M} and Dsx^{M} in mediating the effects of social experience on
580 additional behaviors known to be under circadian control, such as sleep and locomotion. We discovered
581 that the Or47b circuits influence the social modulation of locomotion and courtship behaviors in isolated
582 and grouped flies, respectively, correlating with changes in genes that mediate these behaviors in $Or47b^{2/3}$

583 mutant brains. Importantly, we identified the different effects of Or47b and Or67d pheromone circuits and
584 how they interact with the functions of Fru^M and Dsx^M to regulate their target genes under various social
585 conditions. Given that the regulation of circadian gene networks is complex and participates in the
586 modulation of various behaviors through changes in arousal states, understanding the diverse impacts of
587 Fru^M and Dsx^M on social modulation of target circadian gene expression in the brain is both important and
588 challenging. Fru^M, Dsx^M, and various circadian genes are expressed in different neuronal and non-
589 neuronal (glial and fat body) cell populations in the brain in different combinations. The cellular location
590 of social experience-dependent changes in Fru^M and Dsx^M function and target gene expression remains
591 unknown. Further studies are essential to identify the specific cells in which Fru^M and Dsx^M mediate
592 transcriptional differences in circadian genes in response to social experience. We anticipate that these
593 studies will provide a clearer understanding of how social experience modifies the complex gene
594 regulatory networks for circadian genes downstream of Fru^M and Dsx^M and how these modifications alter
595 behaviors.

596 Overall, our study uncovers how social experience alters transcription and chromatin states in the brain,
597 and provides insights into the roles played by pheromone circuits and transcription factors that influence
598 molecular and behavioral responses to social experience. In addition to modulating behavioral responses,
599 social experience and circadian pathways also influence many physiological responses. These are clearly
600 represented in our transcriptome dataset as social experience-dependent DEGs implicated in immune
601 responses, metabolism, signal transduction, homeostasis, and developmental pathways. The activity of
602 pheromone circuits, along with the functions of Fru^M and Dsx^M, may also play a role in how social
603 experience influences physiological responses through changes in downstream target genes. Future
604 studies will reveal how social experience impacts additional behavioral and physiological responses, and
605 the effects of different pheromone circuits (from both olfactory and gustatory systems), as well as
606 transcriptional and circadian pathways, on these responses.

607

608 # Methods

609 ## Drosophila strains and husbandry

610 Flies were raised on standard fly food from Archon Scientific Company at room temperature. Male flies
611 used in all experiments were 7-day-old. For male-female single-pair courtship behavior assays, unmated
612 males were used as the test fly, and 6-day-old w^{1118} virgin females were used as the target fly. Specific
613 genotypes are listed here (Tweedie et al., 2009): wild-type *CS* (*Canton-S*), *Or47b* mutant (w^+/Y;
614 $Or47b^{2/3}$;+/+) (Wang et al., 2011), *Or67d* mutant (w^+/Y; +/+; $Or67d^{GAL4/GAL4}$) (Kurtovic et al., 2007), *fru*
615 mutant (w^+/Y; +/+; $fru^{LexA/4-40}$) (Anand et al., 2001; Mellert et al., 2010), and *dsx* mutant (w^-/Y; +/+;
616 $dsx^{f00683-d07058/f01649-d09625}$) (Chatterjee et al., 2011).

617 ## Social isolation and group housing setup

618 Dark pupae (80–100 hours old) were picked out and separated by sex. For the social isolation (single
619 housing, SH) condition, each pupa was placed into individual vials, allowed to eclose alone, and aged to 7
620 days. For the group housing (GH) condition, more than 30 pupae of the same sex were collected and
621 placed into food vials, and 30 newly eclosed and unmated flies with correct genotypes were collected and
622 put in a fresh new vial the next day of the collection day (day 0). All w^{1118} virgin females used for the
623 courtship assay were raised under GH conditions.

624 ## Bulk tissue RNA sequencing

625 **Brain dissection and RNA extraction:** Fly brains were dissected in cold RNase-free 1X PBS and
626 transferred immediately to RNAlater (Sigma-Aldrich, R0901) on ice. Each genotype under the GH or SH
627 conditions has three biological replicates, and each biological replicate contains 30 male fly brains. After
628 the dissection, RNAlater with the sample was diluted 1:2 with 1X RNase-free PBS and centrifuged for 1
629 min at max speed, and the supernatant was removed. Brain samples were washed with 1 mL 1X RNase-
630 free PBS and centrifuged for 1 min at max speed. The supernatant was removed and replaced with 300 µL
631 of TRIzol reagent (Invitrogen, 15596026). To extract RNA, samples were ground sufficiently and
632 processed with QIAGEN Shredder kit (QIAGEN, 79654), and RNeasy Mini Kit (QIAGEN, 74104).
633 DNase I (TURBO DNA-free Kit, Invitrogen, Thermo Fisher Scientific AM1907) was applied to remove
634 genomic DNA after the RNA extraction.

635 **Library preparation and sequencing:** Around 500 ng total RNA in each sample was prepared for
636 library preparation. KAPA Stranded mRNA-Seq Kit was used to generate mRNA libraries. Libraries were
637 sequenced on the NextSeq 2000 sequencer, generating 75-bp or 100-bp paired-end reads.

638 **Bulk RNA sequencing data analysis:** Raw fastq files were processed with the standard nf-core/rnaseq
639 pipeline (Ewels et al., 2020). Briefly, reads were mapped to the *Drosophila melanogaster* BDGP6.46
640 genome with STAR, and read counts were generated using the Salmon method. The following analysis
641 was performed in R (R Core Team, 2013; Wickham and Sievert, 2009). DEG analysis was performed
642 with DESeq2 (Love et al., 2014). All control and mutant samples were incorporated into a single
643 DESeqDataSet (dds) object for differential expression analysis. The Wald test was applied to the
644 comparison between GH and SH of the same genotype, and the comparison between mutant and *CS* under
645 the same housing conditions. Gene ontology (GO), Reactome, and KEGG analyses were performed using
646 the clusterProfiler library (Yu et al., 2012).

647 **CUT&RUN**

648 **Brain dissociation and chromatin immunoprecipitation:** Fly brains were dissected in dissection buffer
649 (Schneider′s Insect Medium, Sigma-Aldrich S0146 with 1% BSA) and transferred into cold dissection
650 buffer in 1.5 ml tubes on ice. Each genotype under the GH or SH conditions has three biological
651 replicates. For H3K4me3 samples, fifteen male brains were used per sample, and for RNAPolII samples,
652 thirty male brains were used per sample. After completing the dissection, the old dissection buffer was
653 replaced with a fresh one. Collagenase Type I (Gibco, 17018029) stock solution was added directly into
654 samples for a final 2mg/mL concentration. Samples were incubated at 37 °C for 20 minutes. During the
655 incubation, samples were dissociated by gentle pipetting 20-30 times every 7 min with P200. The
656 collagenase solution was removed after centrifugation at 300 xg for 5 min. Cells were washed with wash
657 buffer supplied in CUTANA™ ChIC/CUT&RUN Kit (EpiCypher, 14-1048), and were centrifuged at 300
658 xg for 5 min. The old wash buffer was replaced with fresh wash buffer, and the cells were resuspended
659 and processed according to the instructions in the user manual. 1 ul of antibody (anti-H3K4me3
660 antibodies supplied by the CUT&RUN Kit, and anti-RNAPolII antibody from MilliporeSigma 05-623)
661 was added per sample.

662 **Library preparation and sequencing:** CUTANA™ CUT&RUN Library Prep Kit (EpiCypher, 14-1001,
663 14-1002) was used to prepare libraries. The quality of libraries was examined by the D5000 ScreenTape
664 station. Libraries were sequenced on the NextSeq 2000 sequencer, generating 75-bp paired-end reads.

665 **CUT&RUN data analysis:** Raw fastq files were processed using the standard nf-core/cutandrun pipeline
666 (Ewels et al., 2020). Briefly, reads were trimmed by Trim Galore and aligned to the *Drosophila*
667 *melanogaster* dmel-all-chromosome-r6.45 genome with Bowtie 2. Peak calling was performed by

668 MACS2. The following analysis was performed in R (R Core Team, 2013; Wickham and Sievert, 2009).
669 Counts of peaks were generated by csaw::regionCounts (Lun and Smyth, 2014, 2015). DEP analysis was
670 performed with DESeq2 (Love et al., 2014). All control and mutant samples were incorporated into a
671 single DESeqDataSet (dds) object for DEP analysis. Wald test was applied to the comparison between
672 GH and SH of the same genotype, and the comparison between mutant and *CS* under the same housing
673 conditions. ChIPseeker was used to annotate DNA peaks with genes. Gene ontology (GO), Reactome, and
674 KEGG analyses were performed using the clusterProfiler library (Yu et al., 2012).

675 Quantitative reverse transcription PCR (RT-qPCR)

676 The RT-qPCR protocol was modified based on the previous protocol (Li et al., 2016). For each housing
677 condition, three to four biological replicates were prepared separately, with each replicate containing 15-
678 20 heads from male flies. Heads were dissected at ZT7-ZT8 on fly pads and immediately transferred into
679 300 ul TRIzol (Invitrogen, 15596026) on ice. RNA extraction and DNase treatment were as described
680 above. cDNA was synthesized through reverse transcription reaction using approximately 200 ng of total
681 RNA with the SuperScript IV First-Strand Synthesis Kit (Invitrogen, 18091050) and poly d(T) primers.
682 qPCR was performed using the FastStart Essential DNA Green Master kit (Roche, 06924204001) on
683 LightCycler® 96 instrument (Roche, 05815916001). Primers used are listed in Table 1. The expression
684 level was calculated by the ΔCt method using *TSG101* as the standard gene. The calculation was
685 performed in R. For each genotype, relative expression between GH and SH male flies was compared
686 using two-sided independent t-tests. For each housing condition, differences among genotypes were
687 assessed using one-way ANOVA followed by Tukey's HSD post-hoc test for pairwise comparisons. In
688 both analyses, raw p-values were adjusted for multiple testing across all comparisons using the
689 Benjamini–Hochberg procedure to control the false discovery rate. Adjusted p-values (*p.adj*) were used to
690 determine statistical significance.

691 **Table 1. Primers used in RT-qPCR experiments**

Primer Names (F: Forward; R: Reverse)	Sequences
TSG101 set47 F	TCCCACGAACTCTTATATGCCT
TSG101 set47 R	CGTGGGATACGGTGGAAAGT
Hmt420 set20 F	ACGATCATATCGTCCGATACCT
Hmt420 set20 R	CGATCTTGTCGTTCTTCGACCA
RPS29 set5 F	ATTGGCTTCAAGAAGCTGGACT
RPS29 set5 R	TGTTGCTGCCGGCATACTAAT
cry set46 F	GCCCAAGGAATTTGTTCACGAG
cry set46 R	GACTTCATGGCCAGCATGTTTC
tim set27 F	TCCCAGCATTCATTCCAAGCA
tim set27 R	GCGTGGCAAACTGTGTTATGTG
Clk set26 F	CCGTGCTCCTCCGATCATTG
Clk set26 R	ACCCGTTTGCCTTAGCTCTTC

692

693 Male-female single-pair courtship behavior assay setup and analysis

694 Courtship behavior assays were performed during ZT 7 – ZT 10 as described (Du et al., 2025). Briefly,
695 one unmated male and one virgin w^{1118} female were gently aspirated to each arena of an unused agarose
696 chamber, separated by barriers before the start of the recording. When all flies were loaded, the chamber

was placed under a camera with a stable, consistent light source. Barriers were removed to allow the two flies to meet each other, and video recording was started immediately. The trajectory of each fly was tracked by FlyTracker (Eyjolfsdottir et al., 2014) on MATLAB. Fly identity and the start time of copulation were determined manually. JAABA was trained and used to automatically annotate other courtship behaviors (Kabra et al., 2013). For each courtship behavior video, only the first 10 minutes were used for the scoring of the courtship index (CI) (copulation time included):

CI = (the time a male fly spends on courtship)/(10 min)

Sleep and locomotion behavior assay setup and analysis

Flies were grouped or isolated for 7 days, and then loaded individually into glass tubes containing food. The activity of each fly was monitored using the Drosophila Activity Monitor (DAM) system (TriKinetics, Waltham, MA) at 25 °C under 12-h light-dark (LD) cycles. The DAM system records activity counts $Ct(t)$ (the number of counts each fly passes the beam) every 30 seconds for two days after the loading to capture one full LD cycle.

Sleep is defined as 5 consecutive minutes or longer with no beam passing.

$$S(t) = \begin{cases} 1, if\ S(t-1) = 1\ and\ Ct(t) = 0 \\ 1, if \sum_{i=t}^{t+10} Ct(i) = 0 \\ 0, otherwise \end{cases}$$

Sleep traces (%) were generated by averaging the sleep data over a duration of 60 minutes.

$$Sc(t) = \frac{1}{120} \sum_{i=t-60}^{t+60} S(i) * 100$$

Locomotion traces (counts) were generated by averaging the activity counts over a duration of 60 minutes.

$$Lc(t) = \frac{1}{120} \sum_{i=t-60}^{t+60} Ct(i)$$

Acknowledgements

We would like to thank members of the Volkan lab for discussions and help with the manuscript. We thank Dr. E. Josie Clowney (University of Michigan, Ann Arbor) for kindly sharing their CUT&RUN protocols. We thank Bloomington Stock Center and Flybase for their services.

Funding

This study was supported by the National Institute of Health grant R01 GM146010 and the National Science Foundation award 2006471 to PCV.

Author contributions

Conceptualization: CD and PCV. Investigation: CD, LJ, and SS with the help from SO and SR. Analysis/interpretation of data: CD, JESF, LJ, CDJ, and PCV. Manuscript—original draft: CD and PCV.

Figures

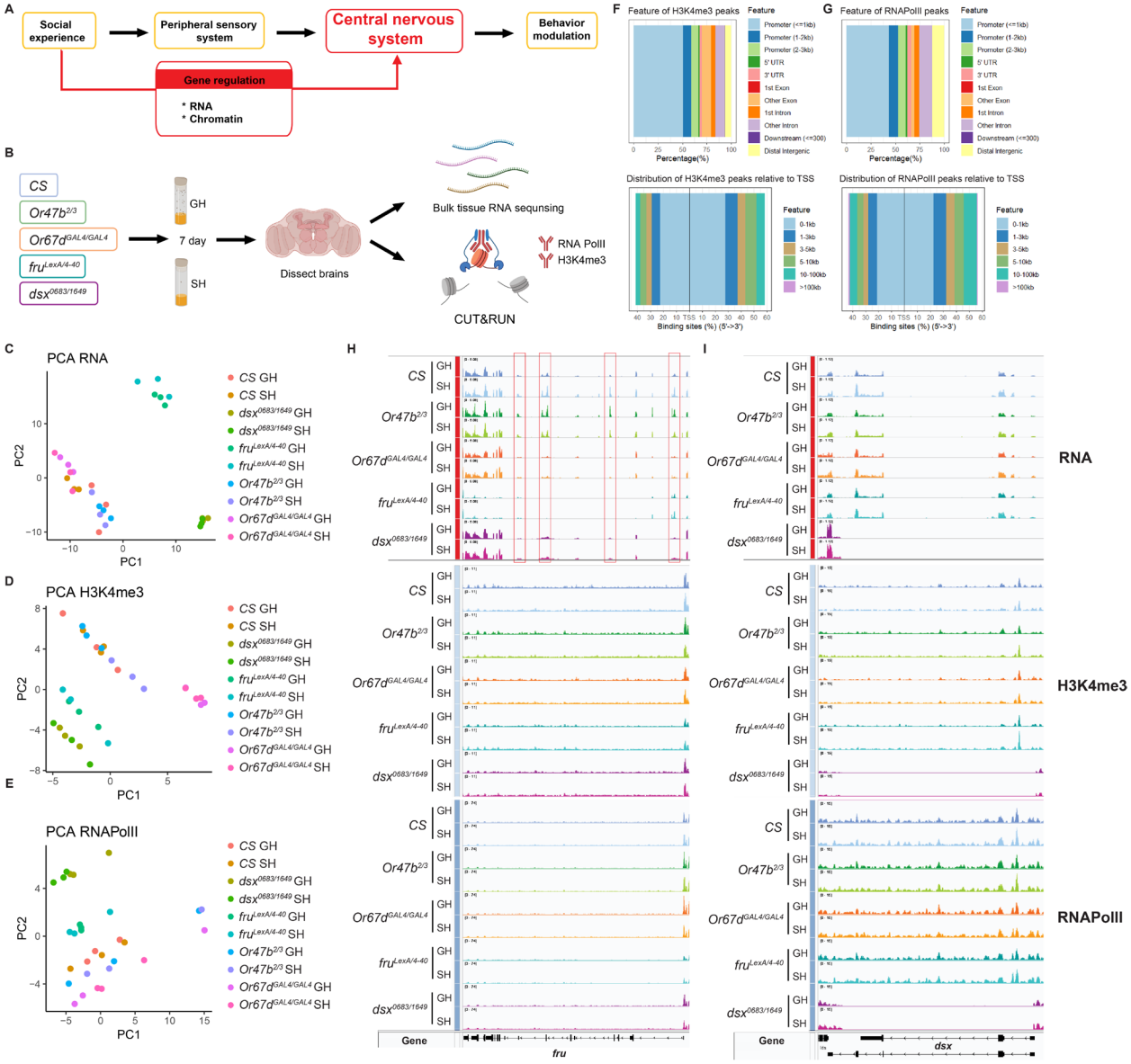

Figure 1. The effect of *Or47b, Or67d, fru^{M}*, and *dsx^{M}* mutants on transcriptional and chromatin states in male brains of GH and SH *Drosophila*. **(A)** Schematic for social signal transduction. **(B)** Brain RNA-seq and CUT&RUN workflow (Created with BioRender). **(C-E)** PCA analysis of transcriptional profiles **(C)**, and H3K4me3 **(D)** and RNAPolII enrichment chromatin profiles **(E)** from GH and SH wild-type *CS*, *Or47b$^{2/3}$*, *Or67d$^{GAL4/GAL4}$*, *fru$^{LexA/4–40}$* and *dsx$^{0683/1649}$* mutant male brains. **(F-G)** Feature distribution of H3K4me3 peaks **(F)** and RNAPolII peaks **(G)**. **(H-I)** IGV view of transcripts, H3K4me3 and RNAPolII distribution around *fru* **(H)** and *dsx* **(I)** locus among all genotypes (three biological replicates overlaid).

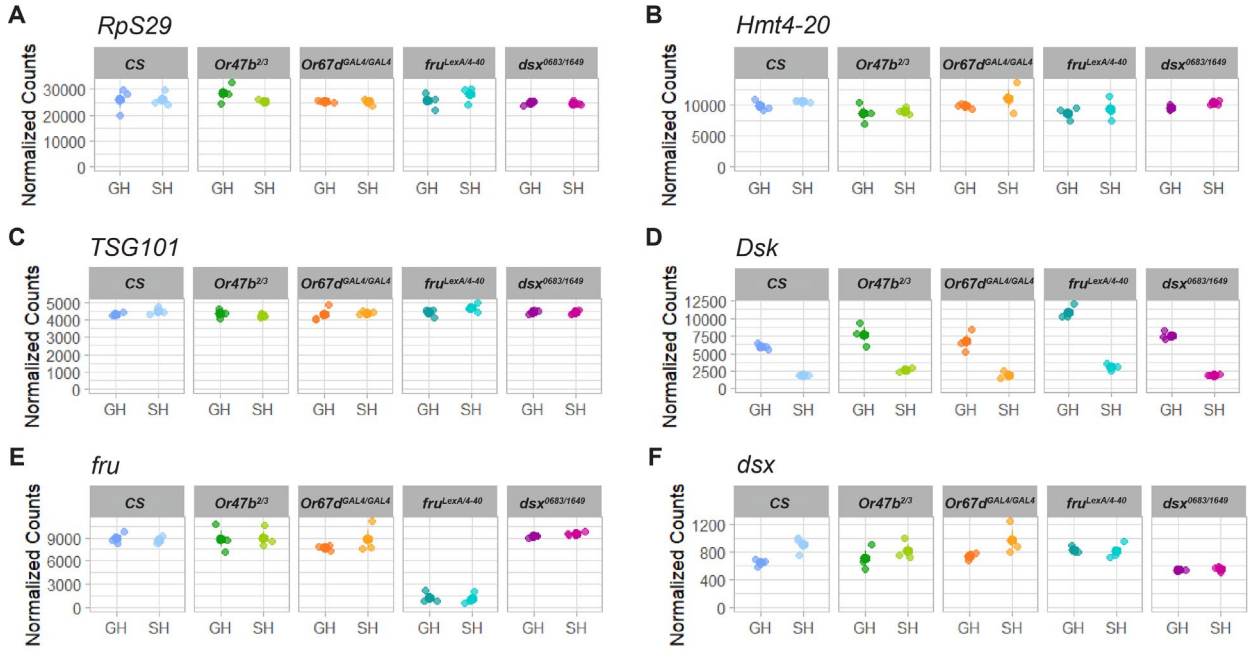

742

743 **Supplementary Figure 1: Normalized counts of genes of interest. (A-F)** Transcript levels for several
744 representative housekeeping genes **(A-C)**, *Dsk* **(D)**, *fru* **(E),** and *dsx* **(F)** among all wild-type and mutant
745 brains.

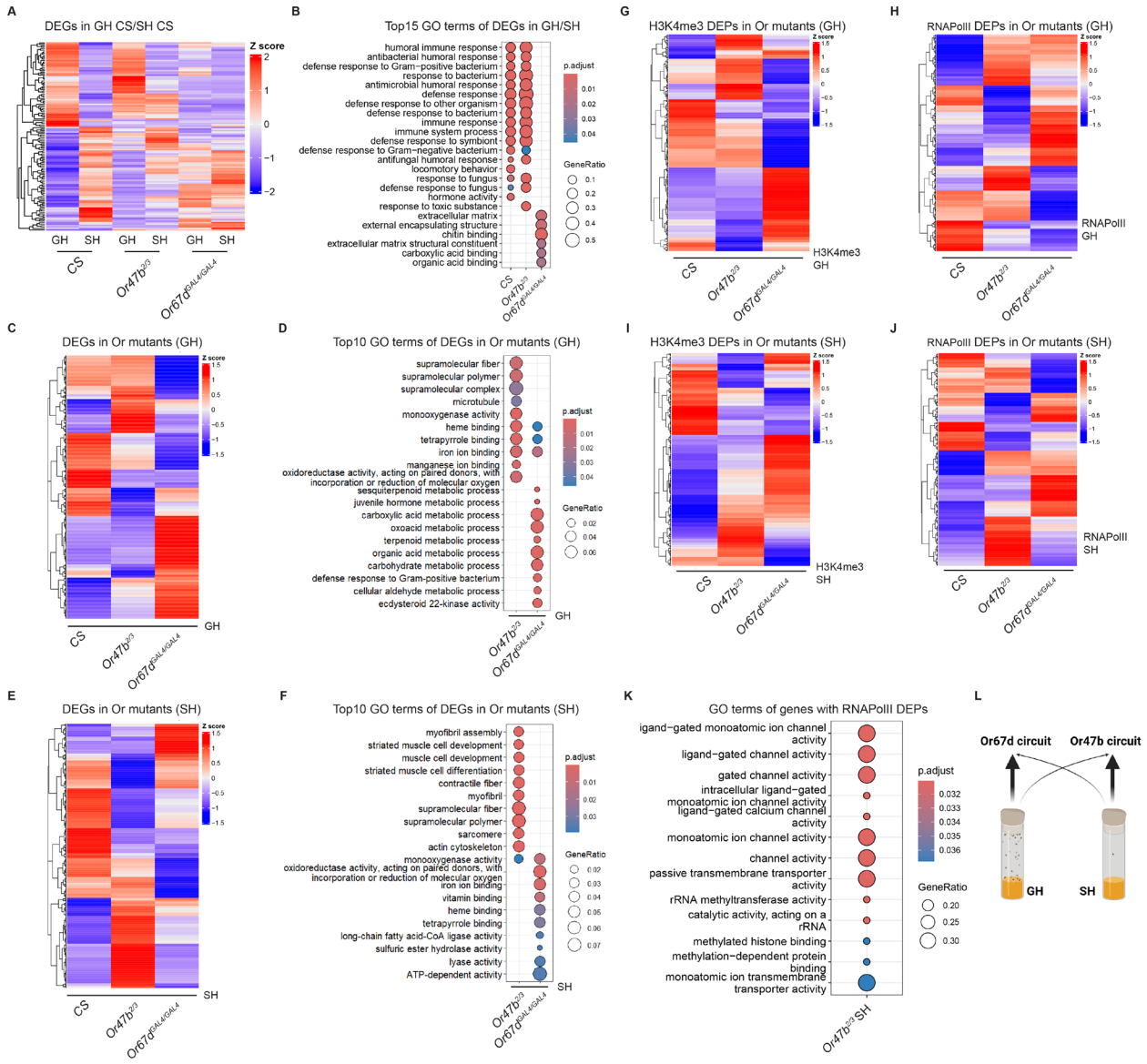

Figure 2. The effect of Or47b and Or67d pheromone circuits on transcriptional and chromatin responses to social experience in the central brain. (A) Heatmaps displaying Z-scores of the median of normalized transcript counts for DEGs identified in the male brains from the GH *CS*/SH *CS* comparison across *CS* and two Or mutants, *Or47b*$^{2/3}$ and *Or67d*$^{GAL4/GAL4}$ (adjusted p-value < 0.05, $|\log_2 FC| > 0.1$). **(B)** Top 15 most significantly enriched GO terms for DEGs of GH/SH comparisons of *CS* and two Or mutants, respectively (q-value < 0.05). **(C, E)** Heatmaps displaying Z-scores of the median of normalized transcript counts for DEGs identified from the Or mutants/*CS* comparison in GH **(C)** and SH **(E)** (adjusted P-value < 0.05, $|\log_2 FC| > 0.1$). **(D, F)** Top 10 most significantly enriched GO terms for DEGs of Or mutants/*CS* comparison in GH **(D)** and SH **(F)** (q-value < 0.05). **(G-H)** Heatmaps displaying Z-scores of the median of normalized enrichment levels of H3K4me3 **(G)** or RNAPolII **(H)** DEPs identified from Or mutants/*CS* comparison in GH brains (adjusted P-value < 0.01). **(I-J)** Heatmaps displaying Z-scores of the median of normalized enrichment levels of H3K4me3 **(I)** or RNAPolII **(J)** DEPs identified from Or mutants/*CS* comparison in SH brains (adjusted P-value < 0.01). **(K)** GO terms for genes with RNAPolII DEPs of *Or47b*$^{2/3}$ mutants/*CS* comparison in SH brains (q-value < 0.05). **(L)** A working model

depicting the roles of Or47b and Or67d pheromone circuits in mediating transcriptional response to social experience in the central brain.

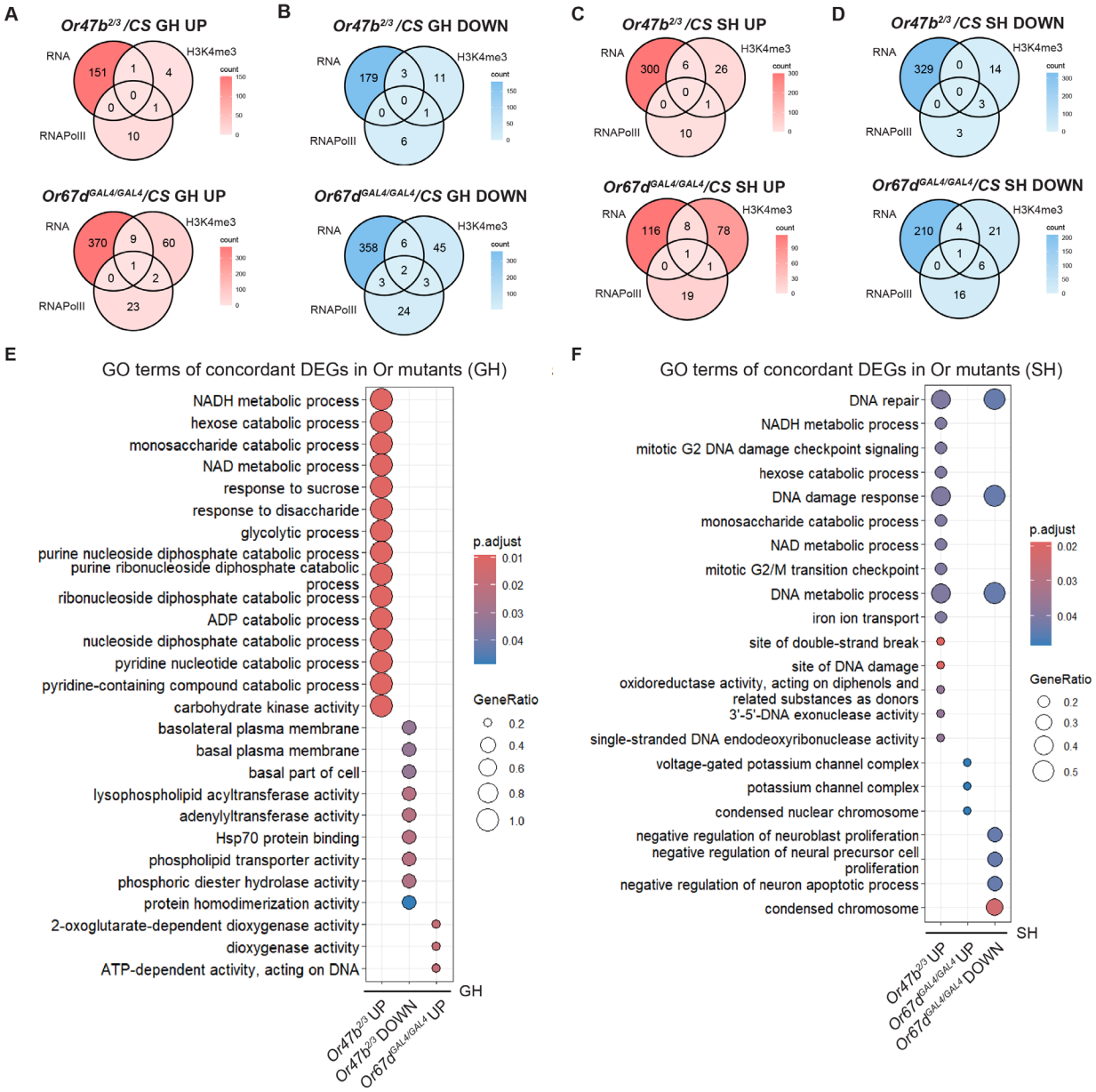

Supplementary Figure 2: Comparisons of DEGs and DEPs in Or mutants. (A-D) Venn diagram comparing DEGs and genes with H3K4me3 or RNAPolII DEPs in the same direction from *Or47b*$^{2/3}$or *Or67d*$^{GAL4/GAL4}$ mutants compared to GH **(A, B)** or SH *CS* **(C, D)**. **(E-F)** GO terms for genes showing concordant changes between transcription and at least one active chromatin mark in Or mutant/*CS* comparisons in GH **(E)** or SH **(F)** male brains (q-value < 0.05).

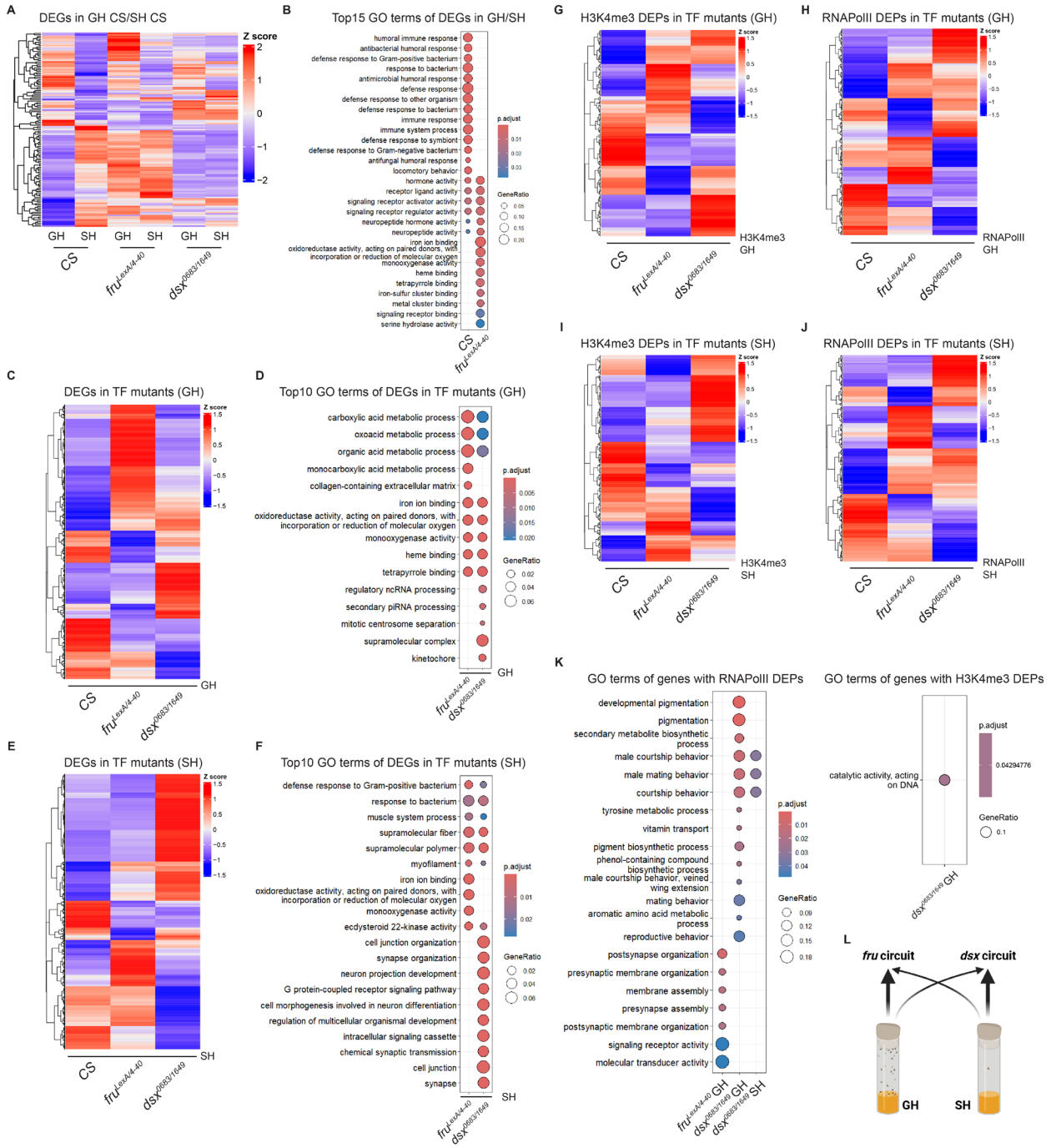

Figure 3. The effect of transcription factors Fru^{M} and Dsx^{M} on transcriptional and chromatin responses to social experience in the central brain. (A) Heatmaps displaying Z-scores of the median of normalized transcript counts for DEGs identified in the male brains from the GH *CS*/SH *CS* comparison across *CS,* and mutants in two transcription factors (TFs), *fru*$^{LexA/4-40}$, and *dsx*$^{0683/1649}$ (adjusted p-value < 0.05, $|\log_2 FC| > 0.1$). **(B)** Top 15 most significantly enriched GO terms for DEGs of GH/SH comparisons of *CS* and *fru*$^{LexA/4-40}$ mutant, respectively (q-value < 0.05). **(C, E)** Heatmaps displaying Z-scores of the median of normalized transcript counts for DEGs identified from TF mutants/*CS* comparison in GH **(C)** and SH **(E)** (adjusted P-value < 0.05, $|\log_2 FC| > 0.1$). **(D, F)** Top 10 most significantly enriched GO terms for DEGs of TF mutants/*CS* comparison in GH **(D)** and SH **(F)** (q-value < 0.05). **(G-H)** Heatmaps

780 displaying Z-scores of the median of normalized enrichment levels of H3K4me3 **(G)** or RNAPolII **(H)**
781 DEPs identified from TF mutants/*CS* comparison in GH brains (adjusted P-value < 0.01). **(I-J)** Heatmaps
782 displaying Z-scores of the median of normalized enrichment levels of H3K4me3 **(I)** or RNAPolII **(J)**
783 DEPs identified from TF mutants/*CS* comparison in SH brains (adjusted P-value < 0.01). **(K)** GO terms
784 for genes with H3K4me3 or RNAPolII DEPs of TF mutants/*CS* comparison in either GH or SH condition
785 (q-value < 0.05). **(L)** A working model displaying the roles of Fru^{M} and Dsx^{M} circuits in mediating
786 transcriptional response to social experience in the central brain.

787

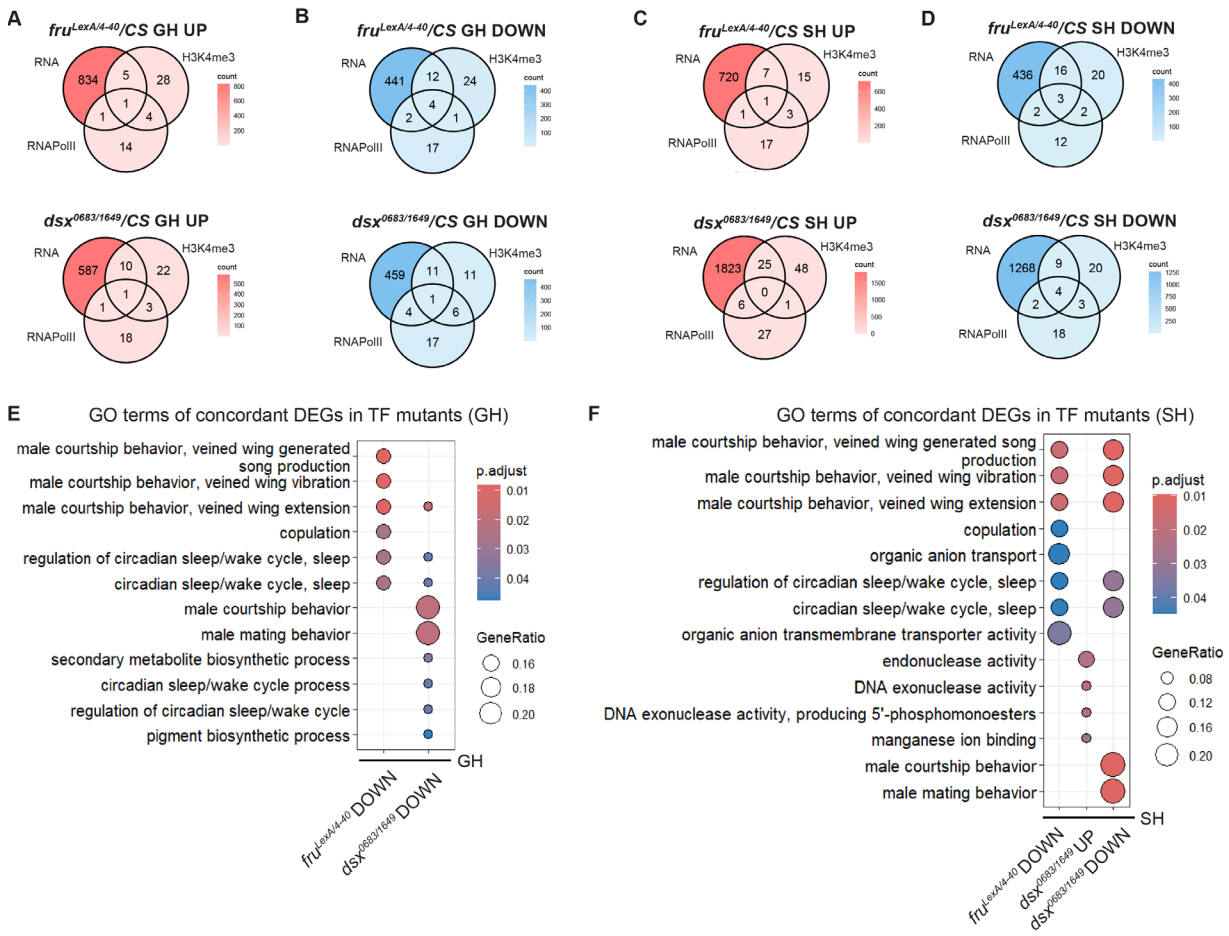

788

789 **Supplementary Figure 3: Comparisons between DEGs and DEPs in TF mutants. (A-D)** Venn
790 diagram comparing DEGs and genes with H3K4me3 or RNAPolII DEPs in the same direction from
791 *fru*$^{LexA/4-40}$ or *dsx*$^{0683/1649}$ mutants compared to GH **(A, B)** or SH *CS* **(C, D)**. **(E-F)** GO terms for genes
792 showing concordant changes between transcription and at least one active chromatin mark in TF
793 mutant/*CS* comparisons in GH **(E)** or SH **(F)** male brains (q-value < 0.05).

794

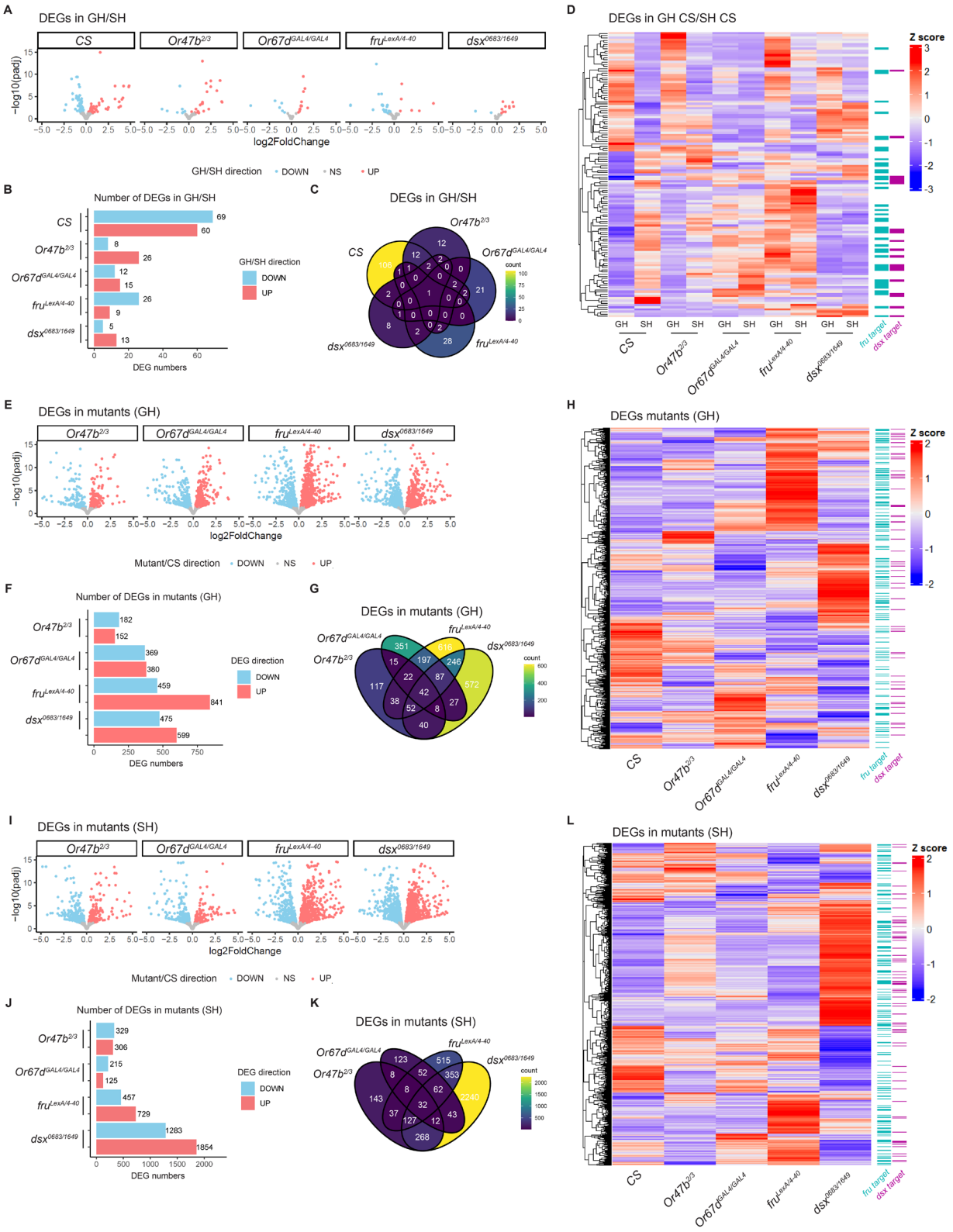

Figure 4: Comparisons of the transcriptional effects of Or and TF mutants in male fly brains. (A) Volcano plots displaying $\log_2$FoldChange (GH/SH) and -log10(p-adj) of genes in each genotype. DEGs

were labeled in red (higher in GH) or blue (lower in GH). **(B)** Numbers of DEGs in GH/SH comparisons for each genotype (adjusted p-value < 0.05, $|\log_2 FC| > 0.1$). **(C)** Venn diagram comparing DEGs from GH/SH comparisons for each genotype. **(D)** Heatmaps displaying Z-scores of the median of normalized transcript counts for DEGs from the GH *CS*/SH *CS* comparison across *CS*, Or mutants, and TF mutants (adjusted p-value < 0.05, $|\log_2 FC| > 0.1$). Putative Fru^M or Dsx^M target genes are labeled on the right. **(E, I)** Volcano plots displaying $\log_2$FoldChange (mutant/*CS*) and -log10(p-adj) of genes in each genotype under GH **(E)** or SH **(I)** condition. DEGs up- and down-regulated in mutants are labeled in red and blue, respectively. **(F, J)** Numbers of DEGs in mutant/*CS* comparisons for each genotype under GH **(F)** or SH **(J)** condition (adjusted p-value < 0.05, $|\log_2 FC| > 0.1$). **(G, K)** Venn diagram comparing DEGs from mutant/*CS* comparisons for each genotype under GH **(G)** or SH **(K)** conditions. **(H, L)** Heatmaps displaying Z-scores of the median of normalized transcript counts for all DEGs from any of the mutant/*CS* comparison under either GH **(H)** or SH **(L)** condition (adjusted p-value < 0.05, $|\log_2 FC| > 0.1$). Putative Fru^M or Dsx^M targets are labeled on the right.

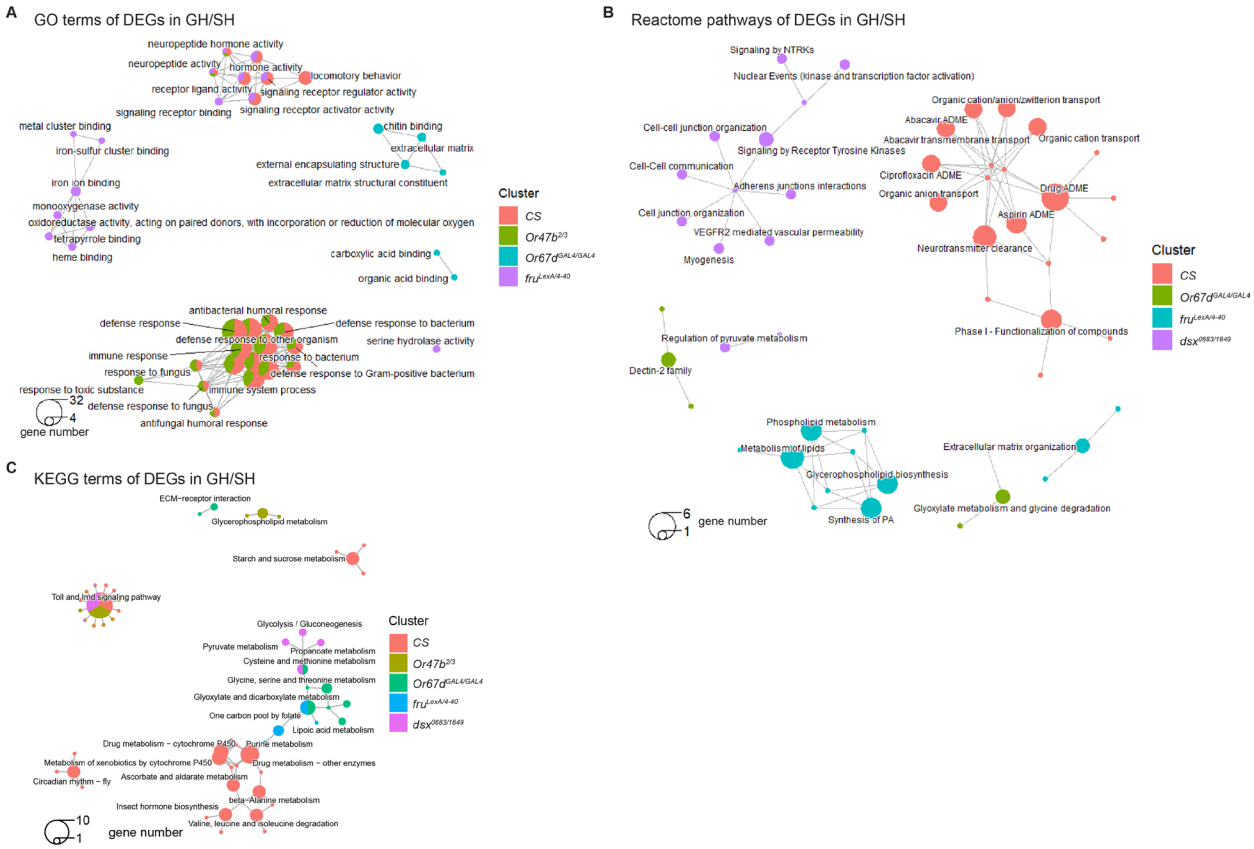

Supplementary Figure 4: GO, Reactome, and KEGG terms of social experience dependent DEGs in *CS*, Or mutants, and TF mutants. (A) Connection plots of the top 15 most significantly enriched GO terms for social experience-dependent DEGs in *CS*, Or mutant, and TF mutant (q-value < 0.05) male brains. **(B)** Connection plots of the top 10 most significantly enriched Reactome pathways for DEGs from GH/SH comparisons of *CS*, Or mutants, and TF mutants (q-value < 0.05). **(C)** Connection plots of the top 10 most significantly enriched KEGG terms for social experience-dependent DEGs in *CS*, Or mutants, and TF mutants (q-value < 0.05).

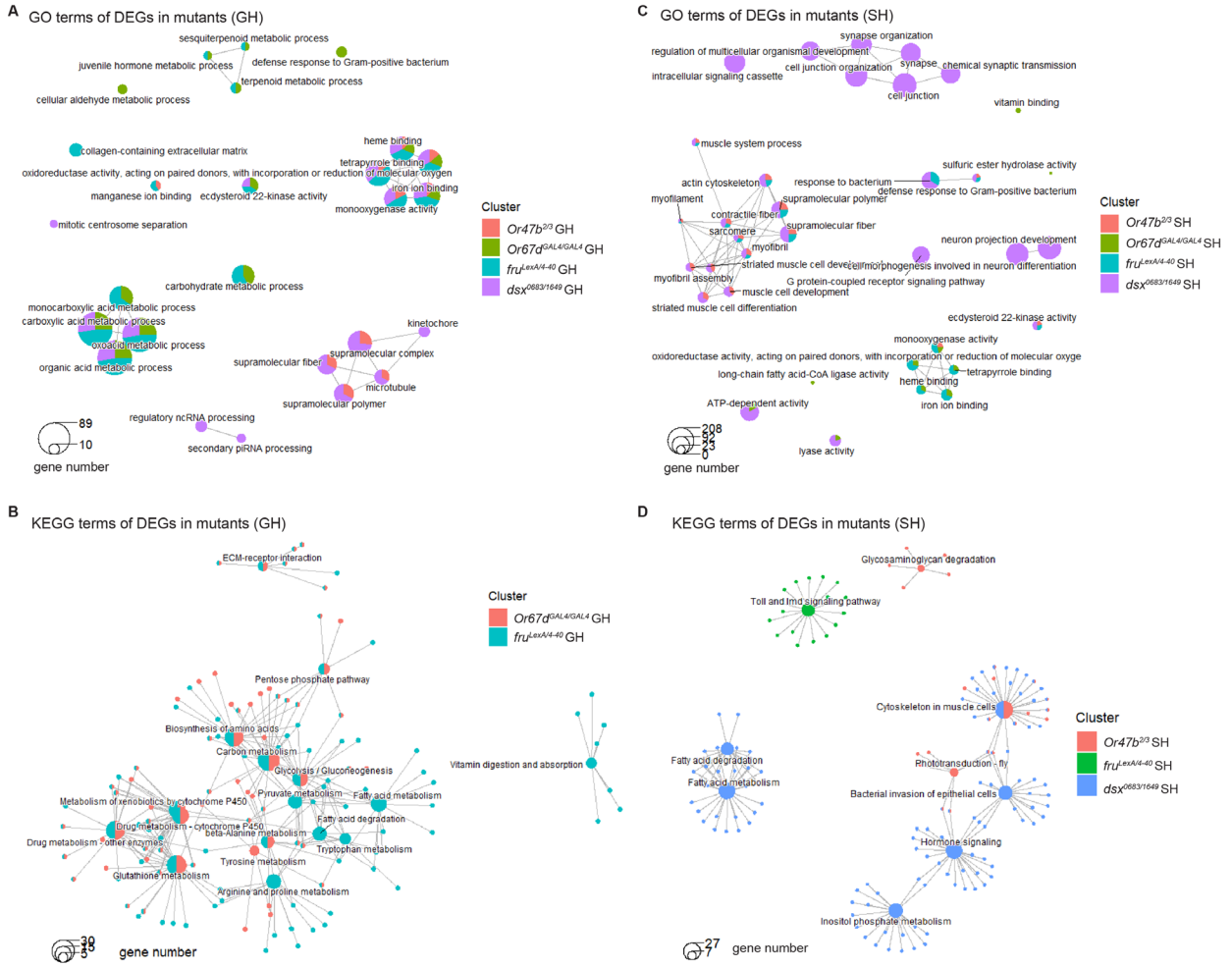

Supplementary Figure 5: GO and KEGG terms from DEGs in mutant/*CS* comparisons. (A, C) Connection plots of the top 10 most significantly enriched GO terms for DEGs from mutant/*CS* comparisons under GH **(A)** or SH **(C)** conditions (q-value < 0.05). **(B, D)** Connection plots of the top 10 most significantly enriched KEGG terms for DEGs from mutant/*CS* comparisons under GH **(B)** or SH **(D)** conditions (q-value < 0.05).

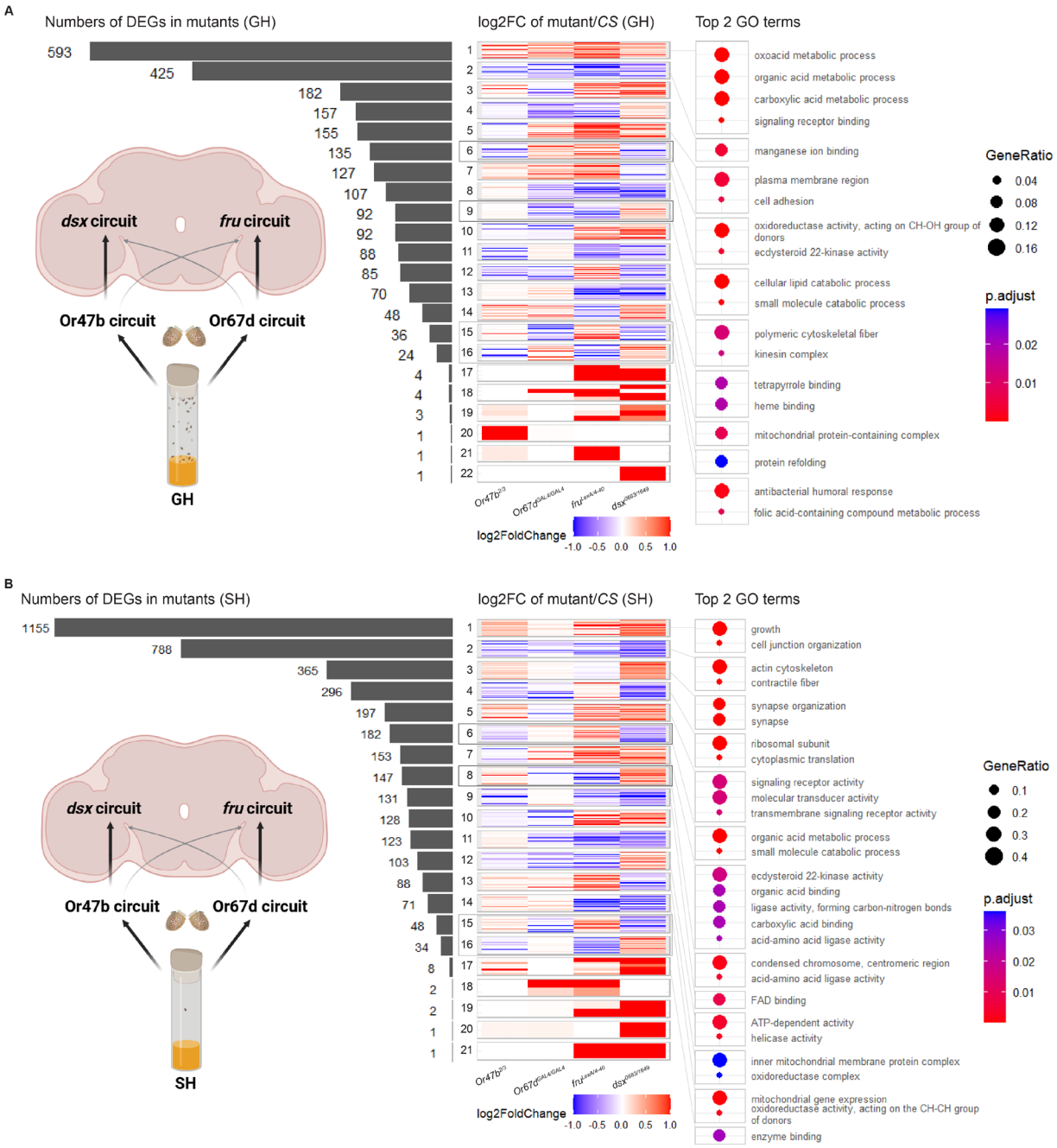

Figure 5: Or47b and Or67d circuits contribute to social modulation of gene expression through the function of Dsx^{M} and Fru^{M}, respectively. (A, B) Bottom left: Models displaying pathways connecting Or47b or Or67d pheromone circuits to *fru* or *dsx* circuits in their transcriptional regulation on male fly brains under GH **(A)** or SH **(B)** condition. Left: Numbers of DEGs in mutant/*CS* comparisons across various combinations of log2FC in different directions. Middle: Heatmaps displaying log2FC of DEGs in mutant/*CS* comparisons across combinations of different directions. Dark gray frames indicate DEGs with log2FC in the same direction between *Or47b*$^{2/3}$and *dsx*$^{0683/1649}$ mutants, as well as between *Or67d*$^{GAL4/GAL4}$ and *fru*$^{LexA/4-40}$ mutants. Light gray frames indicate DEGs with log2FC in the same direction between *Or47b*$^{2/3}$and *fru*$^{LexA/4-40}$ mutants, and between *Or67d*$^{GAL4/GAL4}$ and *dsx*$^{0683/1649}$ mutants. Right: Top 2 GO

837 terms for DEGs in mutant/*CS* comparisons across combinations of log2FC in different directions in the
838 middle.

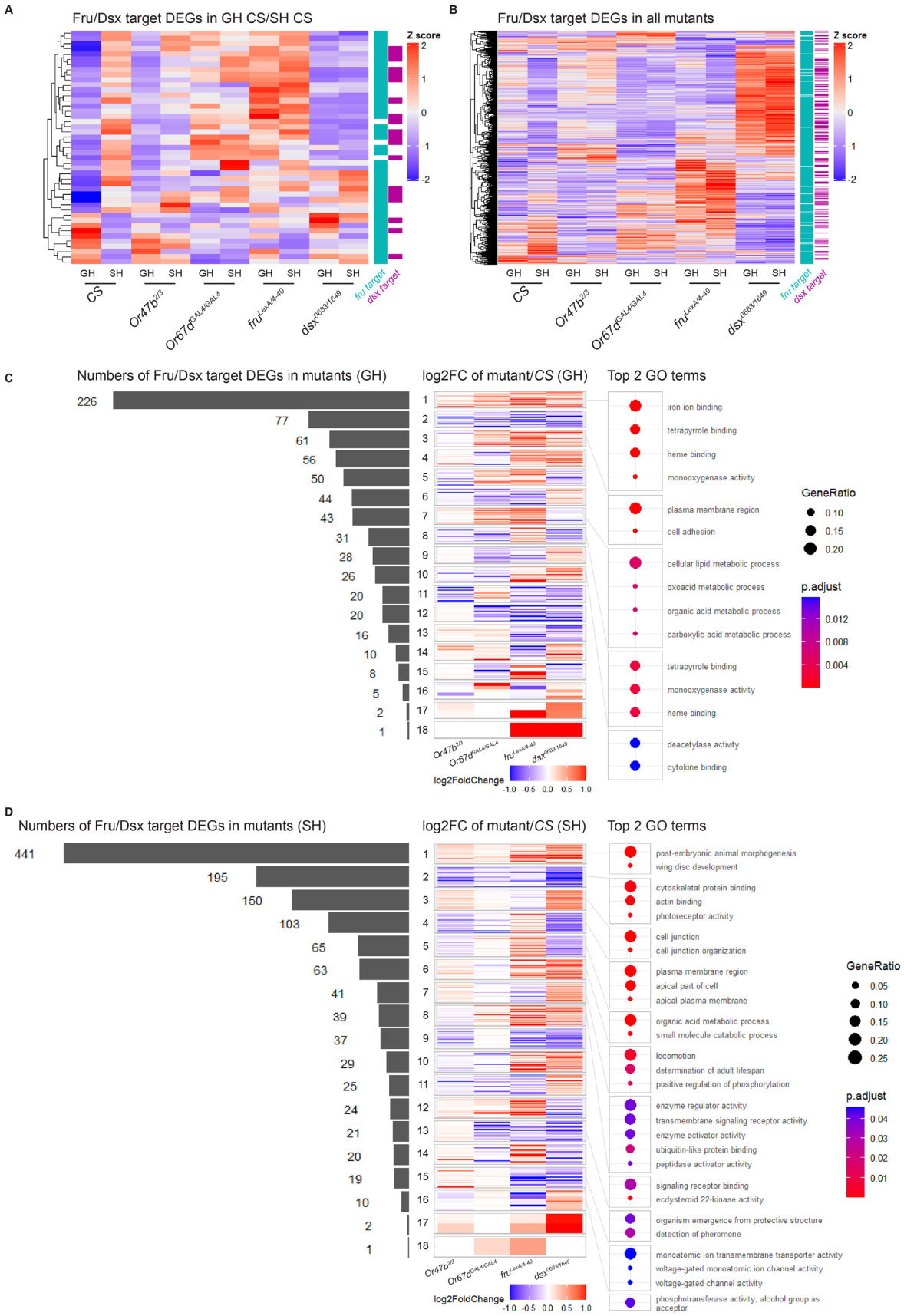
A
Fru/Dsx target DEGs in GH CS/SH CS
Z score
GH SH GH SH GH SH GH SH GH SH
CS
Or47b2/3
Or67dGAL4/GAL4
fruLexA4-40
dsx9683/1649
fru target
dsx target
B
Fru/Dsx target DEGs in all mutants
C
Numbers of Fru/Dsx target DEGs in mutants (GH)
226
77
61
56
50
44
43
31
28
26
20
20
16
10
8
5
2
1
log2FC of mutant/CS (GH)
log2FoldChange
-1.0 -0.5 0.0 0.5 1.0
Top 2 GO terms
iron ion binding
tetrapyrrole binding
heme binding
monooxygenase activity
plasma membrane region
cell adhesion
cellular lipid metabolic process
oxoacid metabolic process
organic acid metabolic process
carboxylic acid metabolic process
tetrapyrrole binding
monooxygenase activity
heme binding
deacetylase activity
cytokine binding
GeneRatio
0.10
0.15
0.20
p.adjust
0.012
0.008
0.004
D
Numbers of Fru/Dsx target DEGs in mutants (SH)
441
195
150
103
65
63
41
39
37
29
25
24
21
20
19
10
2
1
log2FC of mutant/CS (SH)
log2FoldChange
-1.0 -0.5 0.0 0.5 1.0
Top 2 GO terms
post-embryonic animal morphogenesis
wing disc development
cytoskeletal protein binding
actin binding
photoreceptor activity
cell junction
cell junction organization
plasma membrane region
apical part of cell
apical plasma membrane
organic acid metabolic process
small molecule catabolic process
locomotion
determination of adult lifespan
positive regulation of phosphorylation
enzyme regulator activity
transmembrane signaling receptor activity
enzyme activator activity
ubiquitin-like protein binding
peptidase activator activity
signaling receptor binding
ecdysteroid 22-kinase activity
organism emergence from protective structure
detection of pheromone
monoatomic ion transmembrane transporter activity
voltage-gated monoatomic ion channel activity
voltage-gated channel activity
phosphotransferase activity, alcohol group as acceptor
GeneRatio
0.05
0.10
0.15
0.20
0.25
p.adjust
0.04
0.03
0.02
0.01

839

840 **Supplementary Figure 6: Differential effect of pheromone circuits, Fru^M, and Dsx^M on social**
841 **modulation of Fru^M/Dsx^M target gene expression. (A)** Heatmaps displaying Z-scores of the median of
842 normalized transcript counts for Fru^M or Dsx^M target DEGs identified from the GH *CS*/SH *CS*
843 comparison. **(B)** Heatmaps displaying Z-scores of the median of normalized transcript counts for Fru^M or
844 Dsx^M target DEGs identified from the mutant/*CS* comparison under either GH or SH conditions. **(C, D)**
845 Left: Numbers of DEGs in mutant/*CS* comparisons across various combinations of log2FC in different
846 directions under GH **(C)** or SH **(D)** conditions. Middle: Heatmaps displaying log2FC of DEGs in
847 mutant/*CS* comparisons across combinations of different directions. Right: Top 2 GO terms for DEGs in
848 mutant/*CS* comparisons across combinations of log2FC in different directions in the middle.

849

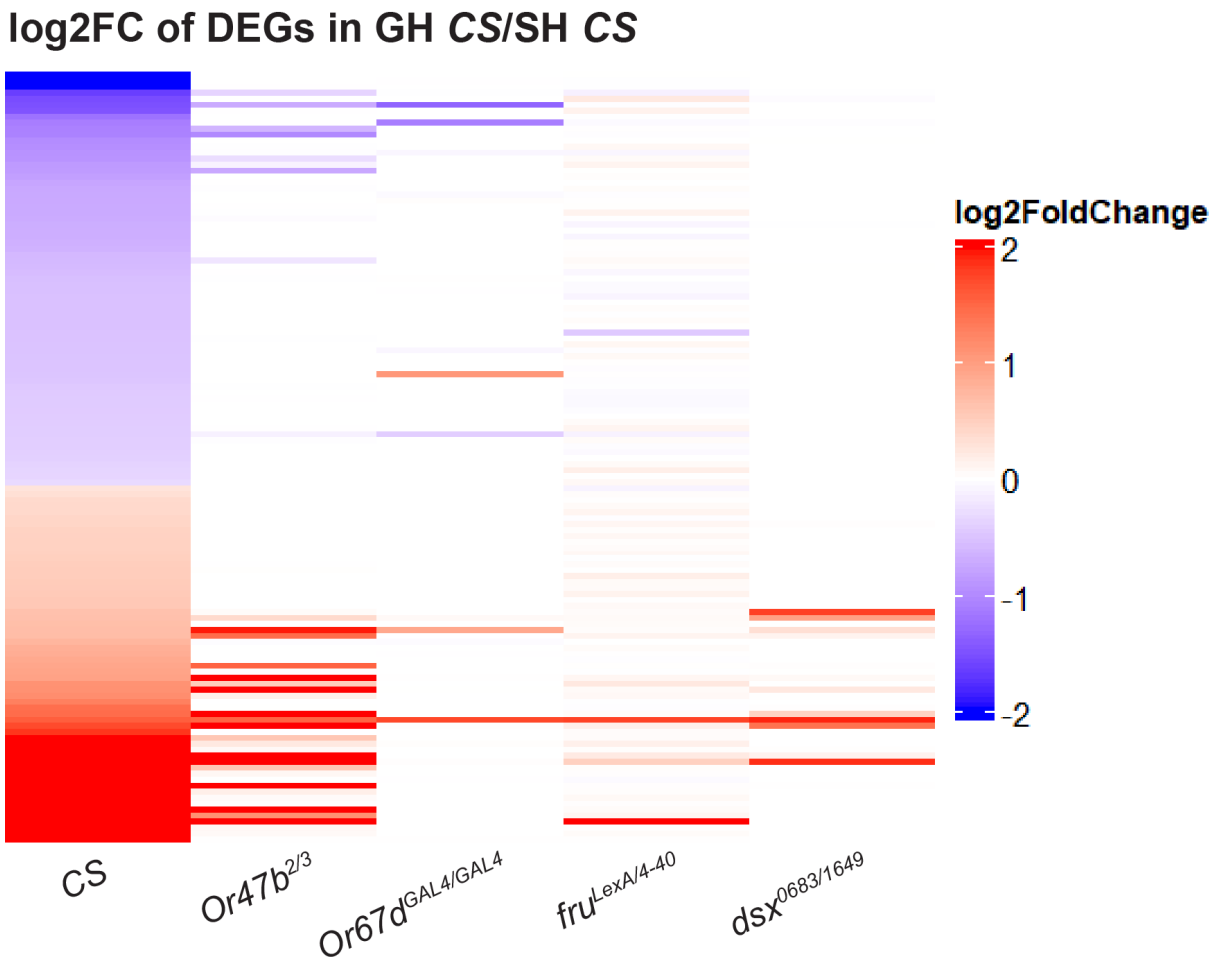

850

851 **Supplementary Figure 7:** Heatmaps displaying log2FC of DEGs from GH *CS*/SH *CS* comparison in all
852 genotypes.

853

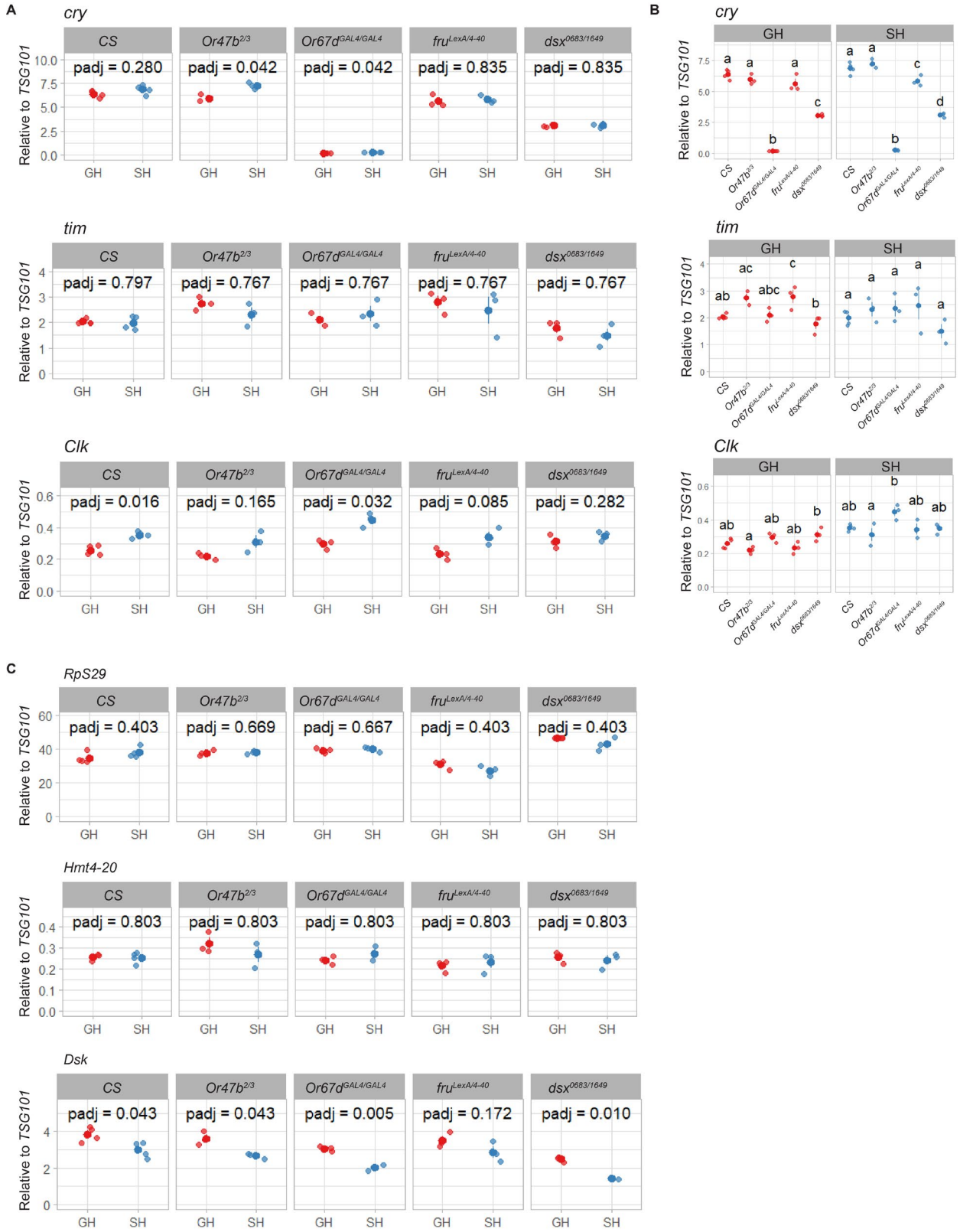
A
cry
CS
Or47b2/3
Or67dGAL4/GAL4
fruLexA/4-40
dsx0683/1649
padj = 0.280
padj = 0.042
padj = 0.042
padj = 0.835
padj = 0.835
tim
padj = 0.797
padj = 0.767
padj = 0.767
padj = 0.767
padj = 0.767
Clk
padj = 0.016
padj = 0.165
padj = 0.032
padj = 0.085
padj = 0.282
Relative to TSG101
GH
SH
B
C
RpS29
padj = 0.403
padj = 0.669
padj = 0.667
padj = 0.403
padj = 0.403
Hmt4-20
padj = 0.803
padj = 0.803
padj = 0.803
padj = 0.803
padj = 0.803
Dsk
padj = 0.043
padj = 0.043
padj = 0.005
padj = 0.172
padj = 0.010

854

855 **Supplementary Figure 8: Expression of circadian genes in male heads in response to social**
856 **experience. (A)** RT-qPCR analysis of *cry*, *tim*, and *Clk* transcript levels in male fly heads between GH
857 and SH across genotypes. Statistical comparisons were performed using two-sided t-tests. P-values were
858 adjusted for multiple comparisons across genotypes using the Benjamini–Hochberg method. **(B)**
859 Comparison of *cry*, *tim*, and *Clk* transcript levels in male fly heads among all genotypes under GH or SH
860 conditions. ANOVA analysis followed by Tukey's HSD test was applied to the statistics. **(C)** Comparison
861 of *RpS29*, *Hmt4-20*, and *Dsk* transcript levels in male fly heads between GH and SH across genotypes.
862 Statistical comparisons were performed using two-sided t-tests. P-values were adjusted for multiple
863 comparisons across genotypes using the Benjamini–Hochberg method.

864

865

866

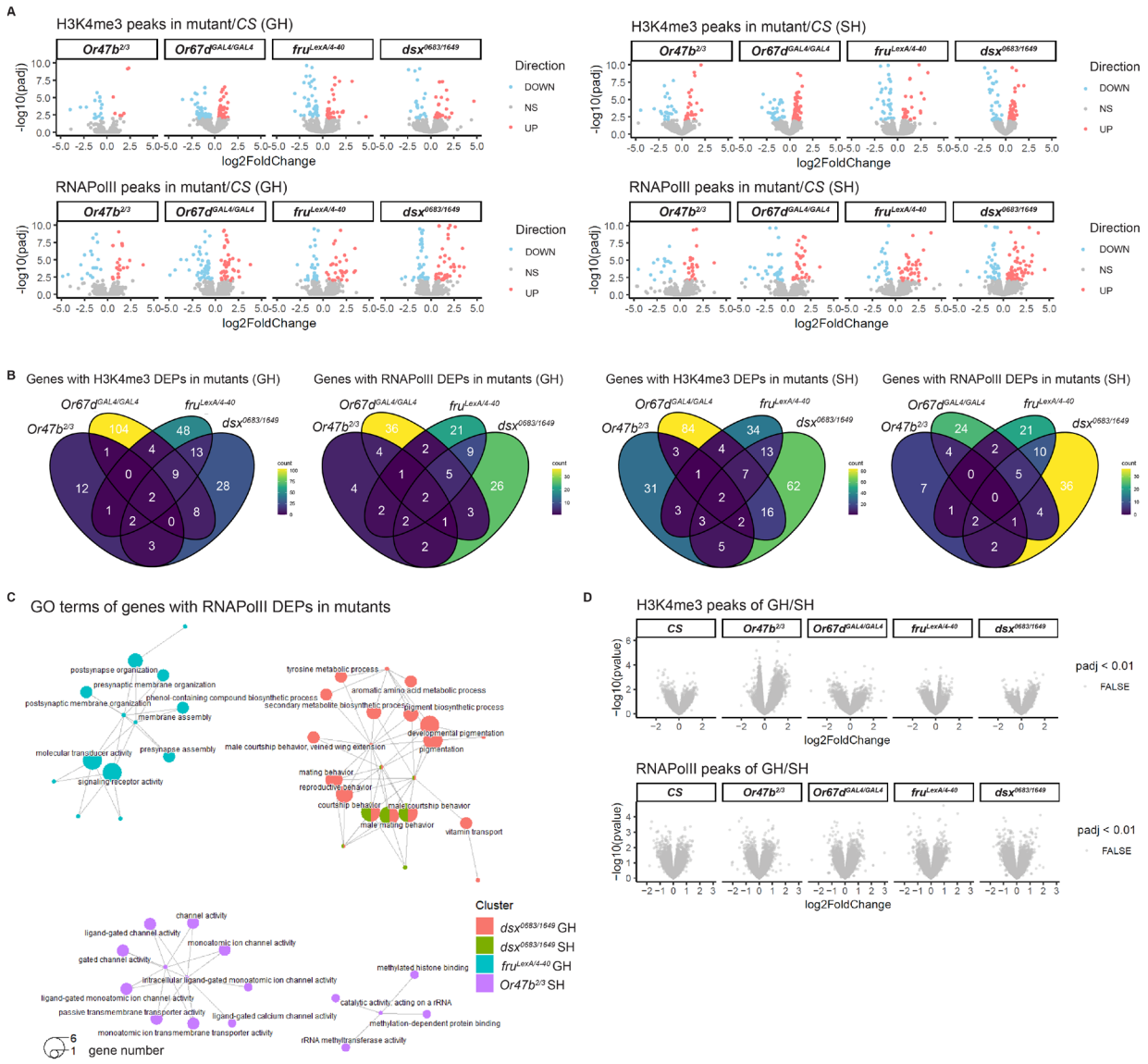

Figure 6: Comparisons of DEPs across Or and TF mutants in male fly brains in different social contexts. (A) Volcano plots showing log2FoldChange and –log10(padj) of mutant/*CS* comparisons for H3K4me3 or RNAPolII peaks under the same housing conditions. Peaks significantly enriched in mutants compared to *CS* are shown in red, while peaks significantly depleted are shown in blue (adjusted p-value < 0.01). **(B)** Venn diagram comparing genes with H3K4me3 or RNAPolII DEPs from mutant/*CS* comparisons under the same housing conditions. **(C)** Connection plots of GO terms for genes with RNAPolII DEPs from mutant/*CS* comparisons (q-value < 0.05). **(D)** Volcano plots showing log2FoldChange (GH/SH) and -log10(p-value) for H3K4me3 and RNAPolII peaks in each genotype. Gray labels peaks with adjusted p-value >= 0.01.

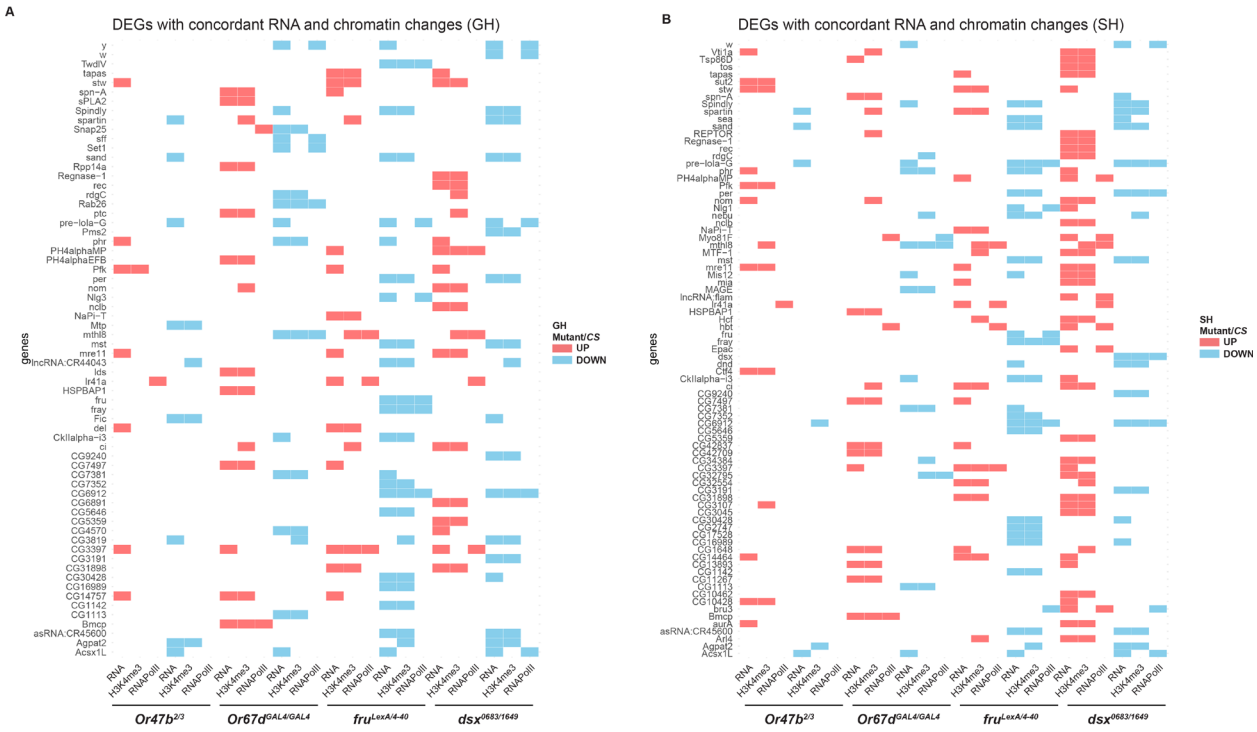

Figure 7: Concordant changes in transcription and chromatin in response to grouping or isolation. **(A, B)** Summary of genes exhibiting concordant changes in transcription and at least one active chromatin mark in each mutant/*CS* comparison under GH **(A)** or SH **(B)** conditions.

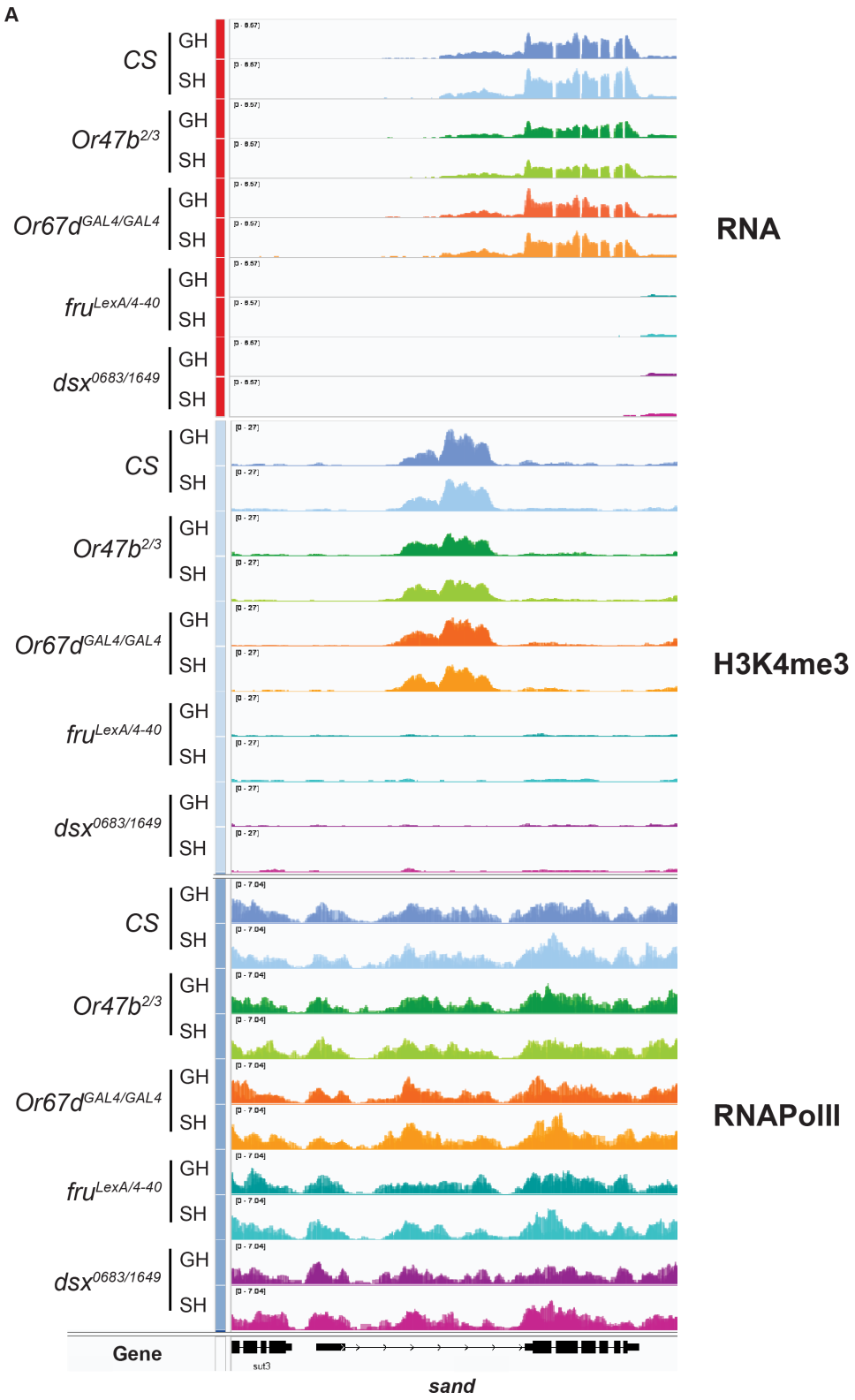

Supplementary Figure 9: Changes in transcript and chromatin marks at the *sand* locus in different mutants and social conditions. IGV tracks showing normalized transcript levels, H3K4me3, and RNAPolII distributions at the *sand* locus across all genotypes (three biological replicates overlaid).

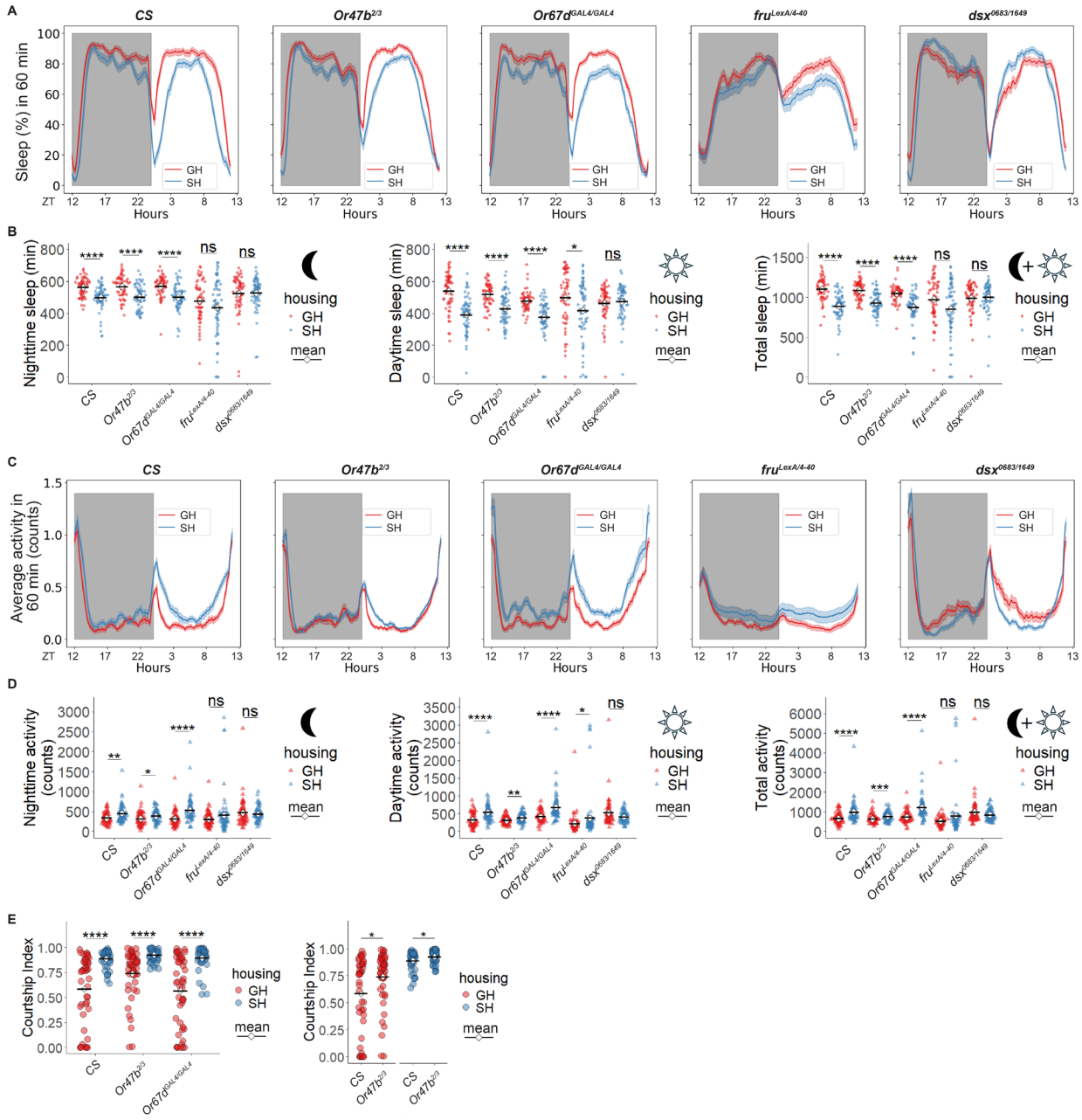

Figure 8: Or47b and Or67d pheromone circuits, Fru^{M}, and Dsx^{M} have differential effects on social modulation of behaviors. (A) Sleep profiles of male flies from each genotype raised under GH or SH conditions, shown as the average proportion of sleep time per 60-minute interval during a 24-hour 12:12 dark-light cycle. Mean ±SEM. **(B)** Quantification of nighttime sleep, daytime sleep, and daily total sleep in **(A)**. Statistical comparisons were performed using the Wilcoxon test. P-values were adjusted for multiple comparisons across genotypes using the Benjamini–Hochberg method. **(C)** Locomotion activity profiles of male flies from each genotype raised under GH or SH conditions, shown as the average counts of beam crossings per 60-minute interval during a 24-hour 12:12 dark-light cycle. Mean ±SEM. **(D)** Quantification of nighttime activity, daytime activity and daily total activity in **(C)**. Statistical comparisons were performed using the Wilcoxon test. P-values were adjusted for multiple comparisons across genotypes using the Benjamini–Hochberg method. *P_adj<0.05, **P_adj<0.01, ***P_adj<0.001, ****P_adj<0.0001. (E) Male-female single pair courtship assay using *CS*, *Or47b*$^{2/3}$, and *Or67d*$^{GAL4/GAL4}$

901 males raised under GH and SH conditions. Statistical comparisons were performed using the Wilcoxon
902 test between GH and SH for each genotype (left) and the comparison between *Or47b*$^{2/3}$ and *CS* under the
903 same housing conditions (right). P-values were adjusted for multiple comparisons across genotypes (left)
904 or housing conditions (right) using the Benjamini–Hochberg method. Significance of adjusted P-value
905 (P_adj): *P_adj < 0.05, **P_adj < 0.01, ***P_adj < 0.001, ****P_adj < 0.0001.

906

907

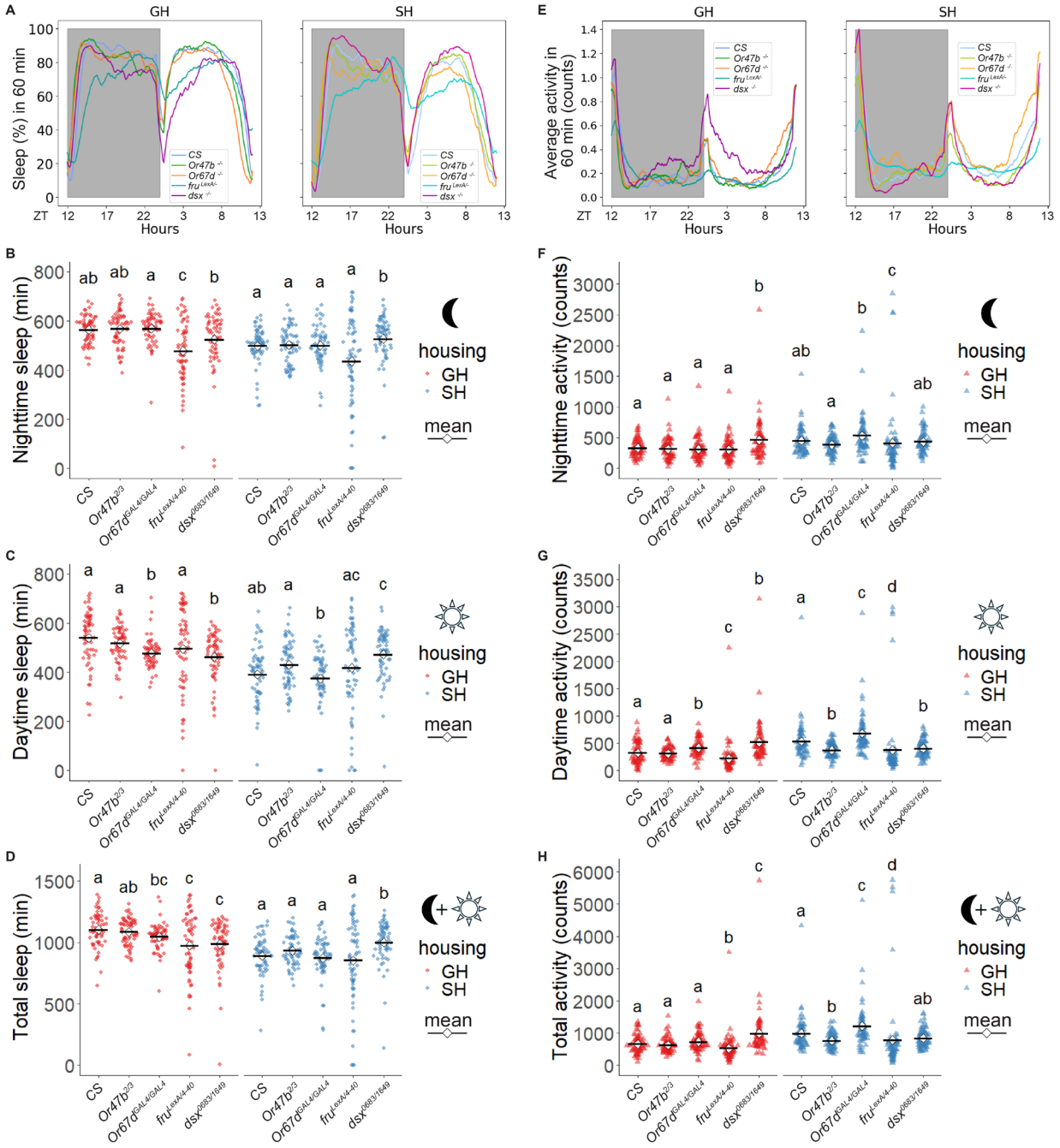

Supplementary Figure 10: Differential effect of Or mutants and TF mutants on social modulation of behaviors. (A) Sleep profiles of male flies from each genotype raised under GH or SH conditions, shown as the average proportion of sleep time per 60-minute interval during a 24-hour 12:12 dark-light cycle. **(B-D)** Quantification of nighttime sleep **(B)**, daytime sleep **(C),** and daily total sleep **(D)** in **(A)**. ANOVA analysis followed by Dunn's test was applied to the statistics. **(E)** Locomotion activity profiles of males from each genotype raised under GH or SH conditions, shown as the average counts of beam crossings per 60-minute interval during a 24-hour 12:12 dark-light cycle. **(F-H)** Quantification of nighttime activity **(F)**, daytime activity **(G),** and daily total activity **(H)** in **(E)**. ANOVA analysis followed

917 by Dunn's test was applied to the statistics. *P_adj<0.05, **P_adj<0.01, ***P_adj<0.001,
918 ****P_adj<0.0001.

919

920 # References

921 Abraham, D.M., Lee, T.E., Watson, L.J., Mao, L., Chandok, G., Wang, H.-G., Frangakis, S., Pitt, G.S.,
922 Shah, S.H., and Wolf, M.J. (2018). The two-pore domain potassium channel TREK-1 mediates cardiac
923 fibrosis and diastolic dysfunction. The Journal of clinical investigation *128*, 4843-4855.

924 Agrawal, P., Chung, P., Heberlein, U., and Kent, C. (2019). Enabling cell-type-specific behavioral
925 epigenetics in Drosophila: a modified high-yield INTACT method reveals the impact of social
926 environment on the epigenetic landscape in dopaminergic neurons. BMC biology *17*, 1-19.

927 Agrawal, P., Kao, D., Chung, P., and Looger, L.L. (2020). The neuropeptide Drosulfakinin regulates
928 social isolation-induced aggression in Drosophila. Journal of Experimental Biology *223*, jeb207407.

929 Anand, A., Villella, A., Ryner, L.C., Carlo, T., Goodwin, S.F., Song, H.-J., Gailey, D.A., Morales, A.,
930 Hall, J.C., and Baker, B.S. (2001). Molecular genetic dissection of the sex-specific and vital functions of
931 the Drosophila melanogaster sex determination gene fruitless. Genetics *158*, 1569-1595.

932 Anders, F. (1978). The effect of social isolation on the aggressive and sexual behaviour in a cichlid fish,
933 Haplochromis burtoni. Behaviour *65*, 43-61.

934 Boros, I.M. (2012). Histone modification in Drosophila. Briefings in functional genomics *11*, 319-331.

935 Brovkina, M.V., Duffié, R., Burtis, A.E., and Clowney, E.J. (2021). Fruitless decommissions regulatory
936 elements to implement cell-type-specific neuronal masculinization. PLoS Genetics *17*, e1009338.

937 Brown, M.K., Strus, E., and Naidoo, N. (2017). Reduced sleep during social isolation leads to cellular
938 stress and induction of the unfolded protein response. Sleep *40*, zsx095.

939 Burtis, K.C., and Baker, B.S. (1989). Drosophila doublesex gene controls somatic sexual differentiation
940 by producing alternatively spliced mRNAs encoding related sex-specific polypeptides. Cell *56*, 997-1010.

941 Cachero, S., Ostrovsky, A.D., Jai, Y.Y., Dickson, B.J., and Jefferis, G.S. (2010). Sexual dimorphism in
942 the fly brain. Current biology *20*, 1589-1601.

943 Cacioppo, J.T., Cacioppo, S., Capitanio, J.P., and Cole, S.W. (2015). The neuroendocrinology of social
944 isolation. Annual review of psychology *66*, 733-767.

945 Cacioppo, J.T., and Hawkley, L.C. (2009). Perceived social isolation and cognition. Trends in cognitive
946 sciences *13*, 447-454.

947 Cacioppo, J.T., Hughes, M.E., Waite, L.J., Hawkley, L.C., and Thisted, R.A. (2006). Loneliness as a
948 specific risk factor for depressive symptoms: cross-sectional and longitudinal analyses. Psychology and
949 aging *21*, 140.

950 Chatterjee, S.S., Uppendahl, L.D., Chowdhury, M.A., Ip, P.-L., and Siegal, M.L. (2011). The female-
951 specific doublesex isoform regulates pleiotropic transcription factors to pattern genital development in
952 Drosophila. Development *138*, 1099-1109.

953 Clough, E., Jimenez, E., Kim, Y.-A., Whitworth, C., Neville, M.C., Hempel, L.U., Pavlou, H.J., Chen, Z.-
954 X., Sturgill, D., and Dale, R.K. (2014). Sex-and tissue-specific functions of Drosophila doublesex
955 transcription factor target genes. Developmental cell *31*, 761-773.

Cohen, S. (2004). Social relationships and health. American psychologist *59*, 676.

Corbett, A.H. (2018). Post-transcriptional regulation of gene expression and human disease. Current opinion in cell biology *52*, 96-104.

Cushing, B.S., and Kramer, K.M. (2005). Mechanisms underlying epigenetic effects of early social experience: the role of neuropeptides and steroids. Neuroscience & Biobehavioral Reviews *29*, 1089-1105.

Dauwalder, B. (2011). The roles of fruitless and doublesex in the control of male courtship. International review of neurobiology *99*, 87-105.

Deanhardt, B., Duan, Q., Du, C., Soeder, C., Morlote, A., Garg, D., Saha, A., Jones, C.D., and Volkan, P.C. (2023). Social experience and pheromone receptor activity reprogram gene expression in sensory neurons. G3: Genes, Genomes, Genetics *13*, jkad072.

Demir, E., and Dickson, B.J. (2005). fruitless splicing specifies male courtship behavior in Drosophila. Cell *121*, 785-794.

Dow-Edwards, D., MacMaster, F.P., Peterson, B.S., Niesink, R., Andersen, S., and Braams, B.R. (2019). Experience during adolescence shapes brain development: From synapses and networks to normal and pathological behavior. Neurotoxicology and teratology *76*, 106834.

Du, C., Okuwa, S., Jia, L., Rozados Barreiro, M., Scott, S., Sotelo Fonseca, J.E., Mabuchi, Y., Appadoo, S., Garcia, L., and Rohrbach, S. (2025). Social experience alters behaviors by reprogramming the Fruitless pathway and circadian state in Drosophila. bioRxiv, 2025.2005. 2030.657129.

Dweck, H.K., Ebrahim, S.A., Thoma, M., Mohamed, A.A., Keesey, I.W., Trona, F., Lavista-Llanos, S., Svatoš, A., Sachse, S., and Knaden, M. (2015). Pheromones mediating copulation and attraction in Drosophila. Proceedings of the National Academy of Sciences *112*, E2829-E2835.

Ewels, P.A., Peltzer, A., Fillinger, S., Patel, H., Alneberg, J., Wilm, A., Garcia, M.U., Di Tommaso, P., and Nahnsen, S. (2020). The nf-core framework for community-curated bioinformatics pipelines. Nature biotechnology *38*, 276-278.

Eyjolfsdottir, E., Branson, S., Burgos-Artizzu, X.P., Hoopfer, E.D., Schor, J., Anderson, D.J., and Perona, P. (2014). Detecting social actions of fruit flies. Paper presented at: Computer Vision–ECCV 2014: 13th European Conference, Zurich, Switzerland, September 6-12, 2014, Proceedings, Part II 13 (Springer).

Flavell, S.W., and Greenberg, M.E. (2008). Signaling mechanisms linking neuronal activity to gene expression and plasticity of the nervous system. Annu Rev Neurosci *31*, 563-590.

Fu, X., Mo, S., Buendia, A., Laurent, A.P., Shao, A., Alvarez-Torres, M.d.M., Yu, T., Tan, J., Su, J., and Sagatelian, R. (2025). A foundation model of transcription across human cell types. Nature, 1-9.

Ganguly-Fitzgerald, I., Donlea, J., and Shaw, P.J. (2006). Waking experience affects sleep need in Drosophila. Science *313*, 1775-1781.

General, O.o.t.S. (2023). Our epidemic of loneliness and isolation: The US Surgeon General's Advisory on the healing effects of social connection and community [Internet].

Glastad, K.M., Graham, R.J., Ju, L., Roessler, J., Brady, C.M., and Berger, S.L. (2020). Epigenetic regulator CoREST controls social behavior in ants. Molecular cell *77*, 338-351. e336.

Goldberg, A.D., Allis, C.D., and Bernstein, E. (2007). Epigenetics: a landscape takes shape. Cell *128*, 635-638.

Goncharova, A., Bragina, Y.V., Fedotov, S., and Kamyshev, N. (2016). Influence of group rearing on sexual behavior of Drosophila melanogaster males. Journal of Evolutionary Biochemistry and Physiology *52*, 454-462.

999 Guerrero, T.P., Fickel, J., Benhaiem, S., and Weyrich, A. (2020). Epigenomics and gene regulation in
1000 mammalian social systems. Current zoology *66*, 307-319.

1001 Ha, T.S., and Smith, D.P. (2006). A pheromone receptor mediates 11-cis-vaccenyl acetate-induced
1002 responses in Drosophila. Journal of Neuroscience *26*, 8727-8733.

1003 Hildreth, P.E. (1965). Doublesex, a recessive gene that tranforms both males and females of Drosophila
1004 into intersexes. Genetics *51*, 659.

1005 Hoffman, H.S., Boskoff, K.J., Eiserer, L.A., and Klein, S.H. (1975). Isolation-induced aggression in
1006 newly hatched ducklings. Journal of Comparative and Physiological Psychology *89*, 447.

1007 Ito, H., Fujitani, K., Usui, K., Shimizu-Nishikawa, K., Tanaka, S., and Yamamoto, D. (1996). Sexual
1008 orientation in Drosophila is altered by the satori mutation in the sex-determination gene fruitless that
1009 encodes a zinc finger protein with a BTB domain. Proceedings of the National Academy of Sciences *93*,
1010 9687-9692.

1011 Ito, H., Sato, K., Koganezawa, M., Ote, M., Matsumoto, K., Hama, C., and Yamamoto, D. (2012).
1012 Fruitless recruits two antagonistic chromatin factors to establish single-neuron sexual dimorphism. Cell
1013 *149*, 1327-1338.

1014 Jai, Y.Y., Kanai, M.I., Demir, E., Jefferis, G.S., and Dickson, B.J. (2010). Cellular organization of the
1015 neural circuit that drives Drosophila courtship behavior. Current biology *20*, 1602-1614.

1016 Jenuwein, T., and Allis, C.D. (2001). Translating the histone code. Science *293*, 1074-1080.

1017 Jeste, D.V., Lee, E.E., and Cacioppo, S. (2020). Battling the modern behavioral epidemic of loneliness:
1018 suggestions for research and interventions. JAMA psychiatry *77*, 553-554.

1019 Kabra, M., Robie, A.A., Rivera-Alba, M., Branson, S., and Branson, K. (2013). JAABA: interactive
1020 machine learning for automatic annotation of animal behavior. Nature methods *10*, 64-67.

1021 Kiani, K., Sanford, E.M., Goyal, Y., and Raj, A. (2022). Changes in chromatin accessibility are not
1022 concordant with transcriptional changes for single-factor perturbations. Molecular systems biology *18*,
1023 e10979.

1024 Kimura, K.-i., Hachiya, T., Koganezawa, M., Tazawa, T., and Yamamoto, D. (2008). Fruitless and
1025 doublesex coordinate to generate male-specific neurons that can initiate courtship. Neuron *59*, 759-769.

1026 Koike, N., Yoo, S.-H., Huang, H.-C., Kumar, V., Lee, C., Kim, T.-K., and Takahashi, J.S. (2012).
1027 Transcriptional architecture and chromatin landscape of the core circadian clock in mammals. science
1028 *338*, 349-354.

1029 Kopp, A. (2012). Dmrt genes in the development and evolution of sexual dimorphism. Trends in Genetics
1030 *28*, 175-184.

1031 Kurtovic, A., Widmer, A., and Dickson, B.J. (2007). A single class of olfactory neurons mediates
1032 behavioural responses to a Drosophila sex pheromone. Nature *446*, 542-546.

1033 Lawrence, M., Daujat, S., and Schneider, R. (2016). Lateral thinking: how histone modifications regulate
1034 gene expression. Trends in Genetics *32*, 42-56.

1035 Lee, G., Foss, M., Goodwin, S.F., Carlo, T., Taylor, B.J., and Hall, J.C. (2000). Spatial, temporal, and
1036 sexually dimorphic expression patterns of the fruitless gene in the Drosophila central nervous system.
1037 Journal of neurobiology *43*, 404-426.

1038 Levine, J.D., Funes, P., Dowse, H.B., and Hall, J.C. (2002). Resetting the circadian clock by social
1039 experience in Drosophila melanogaster. Science *298*, 2010-2012.

1040 Li, Q., Barish, S., Okuwa, S., Maciejewski, A., Brandt, A.T., Reinhold, D., Jones, C.D., and Volkan, P.C.
1041 (2016). A functionally conserved gene regulatory network module governing olfactory neuron diversity.
1042 PLoS genetics *12*, e1005780.

1043 Li, W., Wang, Z., Syed, S., Lyu, C., Lincoln, S., O'Neil, J., Nguyen, A.D., Feng, I., and Young, M.W.
1044 (2021). Chronic social isolation signals starvation and reduces sleep in Drosophila. Nature *597*, 239-244.

1045 Lin, H.-H., Cao, D.-S., Sethi, S., Zeng, Z., Chin, J.S., Chakraborty, T.S., Shepherd, A.K., Nguyen, C.A.,
1046 Yew, J.Y., and Su, C.-Y. (2016). Hormonal modulation of pheromone detection enhances male courtship
1047 success. Neuron *90*, 1272-1285.

1048 Lin, S.L. (2023). The "loneliness epidemic", intersecting risk factors and relations to mental health help-
1049 seeking: A population-based study during COVID-19 lockdown in Canada. Journal of affective disorders
1050 *320*, 7-17.

1051 Liu, D., Rahman, M., Johnson, A., Amo, R., Tsutsui-Kimura, I., Sullivan, Z.A., Pena, N., Talay, M.,
1052 Logeman, B.L., and Finkbeiner, S. (2025). A hypothalamic circuit underlying the dynamic control of
1053 social homeostasis. Nature, 1-11.

1054 Liu, W., Liang, X., Gong, J., Yang, Z., Zhang, Y.-H., Zhang, J.-X., and Rao, Y. (2011). Social regulation
1055 of aggression by pheromonal activation of Or65a olfactory neurons in Drosophila. Nature neuroscience
1056 *14*, 896-902.

1057 Love, M.I., Huber, W., and Anders, S. (2014). Moderated estimation of fold change and dispersion for
1058 RNA-seq data with DESeq2. Genome biology *15*, 1-21.

1059 Luciano, D., and Lore, R. (1975). Aggression and social experience in domesticated rats. Journal of
1060 Comparative and Physiological Psychology *88*, 917.

1061 Lun, A.T., and Smyth, G.K. (2014). De novo detection of differentially bound regions for ChIP-seq data
1062 using peaks and windows: controlling error rates correctly. Nucleic acids research *42*, e95-e95.

1063 Lun, A.T., and Smyth, G.K. (2015). csaw: a Bioconductor package for differential binding analysis of
1064 ChIP-seq data using sliding windows. Nucleic acids research *44*, e45.

1065 Makinodan, M., Rosen, K.M., Ito, S., and Corfas, G. (2012). A critical period for social experience–
1066 dependent oligodendrocyte maturation and myelination. science *337*, 1357-1360.

1067 Matsumoto, K., Pinna, G., Puia, G., Guidotti, A., and Costa, E. (2005). Social isolation stress-induced
1068 aggression in mice: a model to study the pharmacology of neurosteroidogenesis. Stress *8*, 85-93.

1069 McGowan, P.O., Sasaki, A., D'alessio, A.C., Dymov, S., Labonté, B., Szyf, M., Turecki, G., and Meaney,
1070 M.J. (2009). Epigenetic regulation of the glucocorticoid receptor in human brain associates with
1071 childhood abuse. Nature neuroscience *12*, 342-348.

1072 Mellert, D.J., Knapp, J.-M., Manoli, D.S., Meissner, G.W., and Baker, B.S. (2010). Midline crossing by
1073 gustatory receptor neuron axons is regulated by fruitless, doublesex and the Roundabout receptors.
1074 Development *137*, 323-332.

1075 Mikkelsen, T.S., Ku, M., Jaffe, D.B., Issac, B., Lieberman, E., Giannoukos, G., Alvarez, P., Brockman,
1076 W., Kim, T.-K., and Koche, R.P. (2007). Genome-wide maps of chromatin state in pluripotent and
1077 lineage-committed cells. Nature *448*, 553-560.

1078 Murphy, M.W., Zarkower, D., and Bardwell, V.J. (2007). Vertebrate DM domain proteins bind similar
1079 DNA sequences and can heterodimerize on DNA. BMC molecular biology *8*, 1-14.

1080 Nagoshi, R.N., McKeown, M., Burtis, K.C., Belote, J.M., and Baker, B.S. (1988). The control of
1081 alternative splicing at genes regulating sexual differentiation in D. melanogaster. Cell *53*, 229-236.

1082 Neville, M.C., Nojima, T., Ashley, E., Parker, D.J., Walker, J., Southall, T., Van de Sande, B., Marques,
1083 A.C., Fischer, B., and Brand, A.H. (2014). Male-specific fruitless isoforms target neurodevelopmental
1084 genes to specify a sexually dimorphic nervous system. Current Biology *24*, 229-241.

1085 Pan, Y., and Baker, B.S. (2014). Genetic identification and separation of innate and experience-dependent
1086 courtship behaviors in Drosophila. Cell *156*, 236-248.

1087 Pimentel, D., Donlea, J.M., Talbot, C.B., Song, S.M., Thurston, A.J., and Miesenböck, G. (2016).
1088 Operation of a homeostatic sleep switch. Nature *536*, 333-337.

1089 R Core Team, R. (2013). R: A language and environment for statistical computing.

1090 Rideout, E.J., Dornan, A.J., Neville, M.C., Eadie, S., and Goodwin, S.F. (2010). Control of sexual
1091 differentiation and behavior by the doublesex gene in Drosophila melanogaster. Nature neuroscience *13*,
1092 458-466.

1093 Robinett, C.C., Vaughan, A.G., Knapp, J.-M., and Baker, B.S. (2010). Sex and the single cell. II. There is
1094 a time and place for sex. PLoS biology *8*, e1000365.

1095 Robinson, G.E., Fernald, R.D., and Clayton, D.F. (2008). Genes and social behavior. science *322*, 896-
1096 900.

1097 Ryner, L.C., Goodwin, S.F., Castrillon, D.H., Anand, A., Villella, A., Baker, B.S., Hall, J.C., Taylor, B.J.,
1098 and Wasserman, S.A. (1996). Control of male sexual behavior and sexual orientation in Drosophila by the
1099 fruitless gene. Cell *87*, 1079-1089.

1100 Sánchez, M.M., Hearn, E.F., Do, D., Rilling, J.K., and Herndon, J.G. (1998). Differential rearing affects
1101 corpus callosum size and cognitive function of rhesus monkeys. Brain research *812*, 38-49.

1102 Schones, D.E., and Zhao, K. (2008). Genome-wide approaches to studying chromatin modifications.
1103 Nature Reviews Genetics *9*, 179-191.

1104 Sethi, S., Lin, H.-H., Shepherd, A.K., Volkan, P.C., Su, C.-Y., and Wang, J.W. (2019). Social context
1105 enhances hormonal modulation of pheromone detection in Drosophila. Current Biology *29*, 3887-3898.
1106 e3884.

1107 Siuda, D., Wu, Z., Chen, Y., Guo, L., Linke, M., Zechner, U., Xia, N., Reifenberg, G., Kleinert, H., and
1108 Forstermann, U. (2014). Social isolation-induced epigenetic changes in midbrain of adult mice. J Physiol
1109 Pharmacol *65*, 247-255.

1110 Stagkourakis, S., Spigolon, G., Liu, G., and Anderson, D.J. (2020). Experience-dependent plasticity in an
1111 innate social behavior is mediated by hypothalamic LTP. Proceedings of the National Academy of
1112 Sciences *117*, 25789-25799.

1113 Stockinger, P., Kvitsiani, D., Rotkopf, S., Tirián, L., and Dickson, B.J. (2005). Neural circuitry that
1114 governs Drosophila male courtship behavior. Cell *121*, 795-807.

1115 Tung, J., Barreiro, L.B., Johnson, Z.P., Hansen, K.D., Michopoulos, V., Toufexis, D., Michelini, K.,
1116 Wilson, M.E., and Gilad, Y. (2012). Social environment is associated with gene regulatory variation in
1117 the rhesus macaque immune system. Proceedings of the National Academy of Sciences *109*, 6490-6495.

1118 Tweedie, S., Ashburner, M., Falls, K., Leyland, P., McQuilton, P., Marygold, S., Millburn, G., Osumi-
1119 Sutherland, D., Schroeder, A., and Seal, R. (2009). FlyBase: enhancing Drosophila gene ontology
1120 annotations. Nucleic acids research *37*, D555-D559.

1121 Ueda, A., and Kidokoro, Y. (2002). Aggressive behaviours of female Drosophila melanogaster are
1122 influenced by their social experience and food resources. Physiological Entomology *27*, 21-28.

1123 Ueda, A., and Wu, C.-F. (2009). Effects of social isolation on neuromuscular excitability and aggressive
1124 behaviors in Drosophila: altered responses by Hk and gsts1, two mutations implicated in redox regulation.
1125 Journal of neurogenetics *23*, 378-394.

1126 Villella, A., and Hall, J.C. (1996). Courtship anomalies caused by doublesex mutations in Drosophila
1127 melanogaster. Genetics *143*, 331-344.

1128 von Philipsborn, A.C., Jörchel, S., Tirian, L., Demir, E., Morita, T., Stern, D.L., and Dickson, B.J. (2014).
1129 Cellular and behavioral functions of fruitless isoforms in Drosophila courtship. Current Biology *24*, 242-
1130 251.

1131 Vrontou, E., Nilsen, S.P., Demir, E., Kravitz, E.A., and Dickson, B.J. (2006). fruitless regulates
1132 aggression and dominance in Drosophila. Nature neuroscience *9*, 1469-1471.

1133 Wang, L., Han, X., Mehren, J., Hiroi, M., Billeter, J.-C., Miyamoto, T., Amrein, H., Levine, J.D., and
1134 Anderson, D.J. (2011). Hierarchical chemosensory regulation of male-male social interactions in
1135 Drosophila. Nature neuroscience *14*, 757-762.

1136 Wang, Z.Y., McKenzie-Smith, G.C., Liu, W., Cho, H.J., Pereira, T., Dhanerawala, Z., Shaevitz, J.W., and
1137 Kocher, S.D. (2022). Isolation disrupts social interactions and destabilizes brain development in
1138 bumblebees. Current Biology *32*, 2754-2764. e2755.

1139 Weiss, S., Melom, J.E., Ormerod, K.G., Zhang, Y.V., and Littleton, J.T. (2019). Glial Ca2+ signaling
1140 links endocytosis to K+ buffering around neuronal somas to regulate excitability. Elife *8*, e44186.

1141 West, A.E., and Greenberg, M.E. (2011). Neuronal activity–regulated gene transcription in synapse
1142 development and cognitive function. Cold Spring Harbor perspectives in biology *3*, a005744.

1143 Wickham, H., and Sievert, C. (2009). ggplot2: elegant graphics for data analysis, Vol 10 (springer New
1144 York).

1145 Wu, S., Guo, C., Zhao, H., Sun, M., Chen, J., Han, C., Peng, Q., Qiao, H., Peng, P., and Liu, Y. (2019).
1146 Drosulfakinin signaling in fruitless circuitry antagonizes p1 neurons to regulate sexual arousal in
1147 Drosophila. Nat Commun 10: 4770.

1148 Yamagishi, M., Kuze, Y., Kobayashi, S., Nakashima, M., Morishima, S., Kawamata, T., Makiyama, J.,
1149 Suzuki, K., Seki, M., and Abe, K. (2024). Mechanisms of action and resistance in histone methylation-
1150 targeted therapy. Nature *627*, 221-228.

1151 Yamamoto, D., and Koganezawa, M. (2013). Genes and circuits of courtship behaviour in Drosophila
1152 males. Nature Reviews Neuroscience *14*, 681-692.

1153 Yu, G., Wang, L.-G., Han, Y., and He, Q.-Y. (2012). clusterProfiler: an R package for comparing
1154 biological themes among gene clusters. Omics: a journal of integrative biology *16*, 284-287.

1155 Zelikowsky, M., Hui, M., Karigo, T., Choe, A., Yang, B., Blanco, M.R., Beadle, K., Gradinaru, V.,
1156 Deverman, B.E., and Anderson, D.J. (2018). The neuropeptide Tac2 controls a distributed brain state
1157 induced by chronic social isolation stress. Cell *173*, 1265-1279. e1219.

1158 Zhang, Y., Sun, Z., Jia, J., Du, T., Zhang, N., Tang, Y., Fang, Y., and Fang, D. (2021). Overview of
1159 histone modification. Histone Mutations and Cancer, 1-16.

1160 Zhao, H., Jiang, X., Ma, M., Xing, L., Ji, X., and Pan, Y. (2024). A neural pathway for social modulation
1161 of spontaneous locomotor activity (SoMo-SLA) in Drosophila. Proceedings of the National Academy of
1162 Sciences *121*, e2314393121.

1163 Zhao, S., Deanhardt, B., Barlow, G.T., Schleske, P.G., Rossi, A.M., and Volkan, P.C. (2020). Chromatin-
1164 based reprogramming of a courtship regulator by concurrent pheromone perception and hormone
1165 signaling. Science advances *6*, eaba6913.

1166 Zhou, V.W., Goren, A., and Bernstein, B.E. (2011). Charting histone modifications and the functional
1167 organization of mammalian genomes. Nature Reviews Genetics *12*, 7-18.

1168